



# A Posteriori Analysis of the Mixed Finite Element Method for General Second-Order Elliptic Eigenvalue Problems

Shan Nie, Xiaomin Cai, Qiuxia Tian

<sup>1,2,3</sup>(School of Mathematical Sciences, Guizhou Normal University)

Corresponding Author: Shan Nie

**ABSTRACT:** This paper realizes a posteriori analysis for the lowest-order Raviart-Thomas mixed finite element approximation of a class of general second-order elliptic eigenvalue problems. Based on the superconvergence results between the discrete eigenfunctions and the interpolant of eigenfunction, we derive a residual-type error indicator. This error indicator is fully computable and has a clear expression on each element, we verify its reliability and efficiency. Furthermore, we implement adaptive computation, and numerical experiments demonstrate the robustness of the method.

**KEYWORDS:** Second-order elliptic eigenvalues, Raviart-Thomas mixed finite element method, a posteriori analysis, adaptivity

Received 27 Dec., 2024; Revised 05 Jan., 2025; Accepted 07 Jan., 2025 © The author(s) 2025.

Published with open access at [www.questjournals.org](http://www.questjournals.org)

## I. INTRODUCTION

Second-order elliptic eigenvalue problems have garnered significant interest within the scientific community due to their numerous applications across diverse fields, including fluid mechanics, electromagnetism, solid mechanics, and multiphysics field coupling problems. For example, the Raviart-Thomas discretization scheme for second-order elliptic equations and its a priori error estimates are discussed in reference [1]. The application of the Richardson extrapolation method to second-order elliptic eigenvalue problems is studied in reference [2]. The local discontinuous Galerkin method is used to solve the Steklov eigenvalue problem in reference [3].

Using the Raviart-Thomas mixed finite element method to solve general nonsymmetric second-order elliptic eigenvalue problems has also attracted increasing research interest. For example, researchers have discussed posterior error estimates, adaptive algorithms for second-order elliptic eigenvalue problems. As a result, the Raviart-Thomas mixed finite element method has been used to solve various eigenvalue problems, including the Laplace eigenvalue problem, the Stokes eigenvalue problem in fluid mechanics, the eigenvalue problem of Maxwell's equations, and the bi-harmonic eigenvalue problem.

Adaptive finite element methods have been widely applied in various fields. For example, examine superconvergence results based on eigenfunction approximations and analyze residual-type posterior error estimation and adaptive algorithms for second-order elliptic eigenvalue problems in literature [4,5]. A discussion of the adaptive discontinuous finite element method for the convection-diffusion eigenvalue problem in literature [6].

In this paper, a residual type of a posteriori error estimator for the general second order elliptic eigenpair approximation by the mixed finite element method is derived and analyzed, based on a type of superconvergence result of the eigenfunction approximation. Meanwhile, the reliability and effectiveness of the method in eigenfunction computation were verified. The experimental results show that the adaptive algorithm achieves the optimal convergence rate, and the error curve indicates that, for the same degree of freedom, the approximate solution obtained by the adaptive algorithm is more accurate than that of the uniform grid method.

## II. NOTATIONS AND PRELIMINARIES

In this paper, the definitions of some of the symbols used are as follows. We define the Hilbert space

$$H(\operatorname{div}, \Omega) = \left\{ \boldsymbol{\sigma} \in (L^2(\Omega))^2 : \operatorname{div} \boldsymbol{\sigma} \in L^2(\Omega) \right\},$$

equipped with the norm  $\|\sigma\|_{H(div,\Omega)} = (\|\sigma\|_0^2 + \|div\sigma\|_0^2)^{\frac{1}{2}}$

For  $s \geq 0$ , we denote as  $\|\cdot\|_{s,\Omega}$  the norms of the Sobolev space  $L^s(\Omega)$  and  $(L^s(\Omega))^2$ . For scalar fields and vector fields, we define  $H^0(\Omega) = L^2(\Omega)$  and  $(H^0(\Omega))^2 = (L^2(\Omega))^2$ . The corresponding norms are given by

$$\|v\|_{0,\Omega}^2 = \int_{\Omega} |v(x)|^2 dx, \quad \forall v \in L^2(\Omega),$$

$$\|\Psi\|_{0,\Omega}^2 = \int_{\Omega} (\psi_1^2 + \psi_2^2) dx, \quad \forall \Psi \in (L^2(\Omega))^2.$$

In addition, for all vector functions  $\Psi$ , the differential operators are defined as

$$div\Psi = \frac{\partial\psi_1}{\partial x_1} + \frac{\partial\psi_2}{\partial x_2}, \quad rot\Psi = curl\Psi = \frac{\partial\psi_2}{\partial x_1} - \frac{\partial\psi_1}{\partial x_2}.$$

For all scalar functions  $v$ , the differential operators are defined as

$$curlv = \left( \frac{\partial v}{\partial x_2}, -\frac{\partial v}{\partial x_1} \right).$$

Finally, the relation  $a \lesssim b$  indicates that  $a \leq Cb$ , with a positive constant  $C$  which is independent of  $a, b$  and  $\square$ ; Similarly, we define  $a \gtrsim b$  to denote  $a \geq Cb$ , with  $C$  as above.

### III. GENERAL SECOND-ORDER ELLIPTIC EIGENVALUE PROBLEM

$\Omega \subset R^2$  be a bounded domain with Lipschitz boundary  $\partial\Omega$ . and let  $\mathbf{n}$  be the outward normal to  $\partial\Omega$ , consider the Dirichlet boundary condition eigenvalue problem

$$\begin{cases} -div(\nabla u + \mathbf{b}(x)u) + c(x)u = \lambda u, & \text{in } \Omega \\ u = 0, & \text{on } \partial\Omega, \end{cases} \quad (3.1)$$

where  $\mathbf{b}(x)$  and  $c(x)$  are bounded positive functions on  $\Omega$ .

Define the vector-valued function  $\sigma = \nabla u + \mathbf{b}(x)u$ , then problem (3.1) can be equivalently written as

$$\begin{cases} -div\sigma + cu = \lambda u, & \text{in } \Omega \\ \sigma - \nabla u - \mathbf{b} \cdot u = 0, & \text{in } \Omega \\ u = 0, & \text{on } \partial\Omega. \end{cases} \quad (3.2)$$

Next, define the spaces

$$\mathbf{V} = H(div, \Omega), W = L^2(\Omega), G = L^2(\Omega), \mathbf{H} = (L^2(\Omega))^2,$$

then, the weak form for the problem (3.1) can be defined as follows: Find  $(\lambda, \sigma, u) \in C \times \mathbf{V} \times W$ , with  $(\sigma, u) \neq (0,0)$ , such that

$$\begin{cases} a(\sigma, \Psi) - b(\Psi, u) + d(\Psi, u) = 0, \quad \forall \Psi \in \mathbf{V} \\ b(\sigma, v) + e(u, v) = \lambda r(u, v), \quad \forall v \in W, \end{cases} \quad (3.3)$$

where the bilinear forms  $a(\cdot, \cdot), b(\cdot, \cdot), d(\cdot, \cdot), e(\cdot, \cdot)$  and  $r(\cdot, \cdot)$  are defined by

$$\begin{aligned} a(\sigma, \Psi) &= \int_{\Omega} \sigma \cdot \Psi dx, & b(\Psi, v) &= - \int_{\Omega} div\Psi \cdot v dx, & d(\sigma, v) &= - \int_{\Omega} \mathbf{b}\sigma \cdot v dx, \\ e(u, v) &= \int_{\Omega} cuv dx, & r(u, v) &= \int_{\Omega} uv dx. \end{aligned}$$

The bilinear forms  $a(\cdot, \cdot), e(\cdot, \cdot)$  and  $r(\cdot, \cdot)$  are symmetric, and the bilinear forms defined above have the following characteristics:

$$\begin{aligned} |a(\Psi, \Psi)| &\gtrsim \|\Psi\|_{\mathbf{H}}^2, & |e(u, u)| &\geq 0, & |r(u, u)| &\geq 0, \\ |a(\sigma, \Psi)| &\lesssim \|\sigma\|_{\mathbf{H}} \|\Psi\|_{\mathbf{H}}, & |b(\Psi, v)| &\lesssim \|\Psi\|_{\mathbf{V}} \|v\|_W, \\ |d(\Psi, u)| &\lesssim \|\Psi\|_{\mathbf{H}} \|u\|_W, & |e(u, v)| &\lesssim \|u\|_W \|v\|_W, & |r(u, v)| &\lesssim \|u\|_W \|v\|_W. \end{aligned}$$

For the eigenvalue  $\lambda$ , the Rayleigh quotient can be expressed as

$$\lambda = \frac{a(\sigma, \sigma) + d(\sigma, u) + e(u, u)}{r(u, u)}. \quad (3.4)$$

From [7], the sequence of eigenvalues corresponding to the eigenvalue problem (3.3) is given by

$$0 \leq \lambda_1 \leq \lambda_2 \leq \dots \leq \lambda_k \leq \dots, \lim_{k \rightarrow \infty} \lambda_k = \infty,$$

and the associated eigenfunctions

$$(\sigma_1, u_1), (\sigma_2, u_2), \dots, (\sigma_k, u_k), \dots.$$

The global stability result for problem (3.3) can be obtained from [4] as follows.

**Lemma 3.1.** For all  $(\Psi, v) \in \mathbf{V} \times W$ , the following inf-sup condition holds

$$\sup_{0 \neq (\sigma, u) \in \mathbf{V} \times W} \frac{a(\sigma, \Psi) - b(\Psi, u) + d(\Psi, u) + b(\sigma, v) + e(u, v)}{\|\sigma\|_{\mathbf{V}} + \|u\|_W} \gtrsim \|\Psi\|_{\mathbf{V}} + \|v\|_W.$$

### IV. MIXED FINITE ELEMENT METHOD

In this section, we explore approximation methods for the eigenvalue problem (3.3) in mixed finite element method. To define the discrete approximation solution, we first define a shape regular mesh for the

domain  $\Omega$  denoted by  $\mathcal{T}_h = \{\kappa\}$ , where each element  $\kappa$  has edge length  $h_E$  and the diameter  $h_\kappa$ . The mesh size is defined as  $h = \max_{\kappa \in \mathcal{T}_h} h_\kappa$ . This triangulation  $\mathcal{T}_h$  satisfies the following conditions:

- (i) Any two triangles share at most one edge or one vertex;
- (ii) All triangles have a positive lower bound on their lowest interior angle;
- (iii) There exists a constant  $\gamma^*$  such that for any element  $\kappa \in \mathcal{T}_h$ , the following holds

$$\frac{h_\kappa}{\rho_\kappa} \leq \gamma^*, \forall \kappa \in \mathcal{T}_h,$$

where  $\rho_\kappa$  denotes the diameter of the largest inscribed circle of element  $\kappa$ ;

- (iv) For any element  $\kappa \in \mathcal{T}_h$ , let the area of element  $\kappa$  be  $|\kappa|$ , we have

$$C_3 h^2 \leq C_1 h_\kappa^2 \leq |\kappa| \leq C_2 h_\kappa^2 \leq C_4 h^2,$$

where  $C_i (i = 1, 2, 3, 4)$  are constants independent of the mesh size  $h$ , and  $h$  is a positive real number approaching zero.

Additionally, the boundary  $\Gamma_h = \Gamma_h^0 \cup \Gamma_h^\partial$  is divided into two parts:  $\Gamma_h^0$  represents the interior edges, and  $\Gamma_h^\partial$  represents the edges on the boundary  $\partial\Omega$ .

Associated with the partition  $\mathcal{T}_h$ , we define the finite-dimensional spaces  $\mathbf{V}_h$  and  $W_h$  of the lowest order Raviart-Thomas mixed finite element spaces (see [4]), where  $P_m(\kappa)$  denotes the spaces of a polynomial of degree  $\leq m$  on  $\kappa$ .

Define

$$\mathbf{V}_h = \{\boldsymbol{\Psi} \in \mathbf{V}: \boldsymbol{\Psi}|_\kappa \in P_0(\kappa)^2 \oplus (x_1, x_2)^T P_0(\kappa), \forall \kappa \in \mathcal{T}_h\},$$

which clearly implies  $\mathbf{V}_h \subset \mathbf{V}$ .

Afterward, define

$$W_h = \{v \in W: v|_\kappa \in P_0(\kappa), \forall \kappa \in \mathcal{T}_h\},$$

likewise, we have  $W_h \subset W$ , and the connection  $\text{div} \mathbf{V}_h = W_h$  is valid.

With the discrete spaces defined above, we are in position to introduce the discretization of problem (3.3): Find  $(\lambda_h, \boldsymbol{\sigma}_h, u_h) \in \mathcal{C} \times \mathbf{V}_h \times W_h$ , such that

$$\begin{cases} a(\boldsymbol{\sigma}_h, \boldsymbol{\Psi}) - b(\boldsymbol{\Psi}, u_h) + d(\boldsymbol{\Psi}, u_h) = 0, & \forall \boldsymbol{\Psi} \in \mathbf{V}_h \\ b(\boldsymbol{\sigma}_h, v) + e(u_h, v) = \lambda_h r(u_h, v), & \forall v \in W_h. \end{cases} \quad (4.1)$$

From (4.1), the following Rayleigh quotient expression for  $\lambda_h$  also holds

$$\lambda_h = \frac{a(\boldsymbol{\sigma}_h, \boldsymbol{\sigma}_h) + d(\boldsymbol{\sigma}_h, u_h) + e(u_h, u_h)}{r(u_h, u_h)}. \quad (4.2)$$

And from [7] the eigenvalue problem (4.1) has eigenvalues

$$0 \leq \lambda_{1,h} \leq \lambda_{2,h} \leq \dots \leq \lambda_{k,h} \leq \dots \leq \lambda_{N,h},$$

and the corresponding eigenfunctions

$$(\boldsymbol{\sigma}_{1,h}, u_{1,h}), (\boldsymbol{\sigma}_{2,h}, u_{2,h}), \dots, (\boldsymbol{\sigma}_{k,h}, u_{k,h}), \dots, (\boldsymbol{\sigma}_{N,h}, u_{N,h}),$$

where  $N$  is the dimension of the mixed finite element space  $\mathbf{V}_h \times W_h$ .

In this paper, we use  $\mathbf{P}_h: \mathbf{V} \rightarrow \mathbf{V}_h$  and  $Q_h: W \rightarrow W_h$  to denote the Raviart-Thomas interpolation operators which are defined by the following conditions:

- (i) For each edge  $E_i (i = 1, 2, 3)$  of any triangular element  $\kappa \in \mathcal{T}_h$ , the following condition holds

$$\int_{E_i} (\boldsymbol{\sigma} - \mathbf{P}_h \boldsymbol{\sigma}) \cdot \mathbf{n}_i ds = 0, \quad (4.3)$$

where  $\mathbf{n}_i (i = 1, 2, 3)$  is the unit outward normal vector on the edge  $E_i$ ;

- (ii) For each element  $\kappa$ , the following condition applies

$$\int_\kappa (u - Q_h u) dx = 0; \quad (4.4)$$

- (iii) The interpolation operators satisfy the following relation

$$\text{div} \mathbf{P}_h = Q_h \text{div}. \quad (4.5)$$

We also need to define the mixed finite element projection operator  $(\boldsymbol{\Pi}_h, \Sigma_h): \mathbf{V} \times W \rightarrow \mathbf{V}_h \times W_h$ , for any  $(\boldsymbol{\sigma}, u) \in \mathbf{V} \times W$  such that

$$\begin{cases} a(\boldsymbol{\Pi}_h \boldsymbol{\sigma} - \boldsymbol{\sigma}, \boldsymbol{\Psi}_h) - b(\boldsymbol{\Psi}_h, \Sigma_h u - u) + d(\boldsymbol{\Psi}_h, \Sigma_h u - u) = 0, & \forall \boldsymbol{\Psi}_h \in \mathbf{V}_h \\ b(\boldsymbol{\Pi}_h \boldsymbol{\sigma} - \boldsymbol{\sigma}, v_h) + e(\Sigma_h u - u, v_h) = 0, & \forall v_h \in W_h. \end{cases} \quad (4.6)$$

For this type of projection, we have the following estimate (see [1,8]):

$$\|\boldsymbol{\sigma} - \boldsymbol{\Pi}_h \boldsymbol{\sigma}\|_V \lesssim h \|\boldsymbol{\sigma}\|_1, \quad \|u - \Sigma_h u\|_0 \lesssim h \|u\|_1. \quad (4.7)$$

Next, define the linear bounded operators  $T$  and  $\mathbf{S}$ , as well as their discrete versions  $T_h$  and  $\mathbf{S}_h$ :

$$\begin{aligned} T: G &\rightarrow W \subset G, & Tg &= u, \\ T_h: G &\rightarrow W_h \subset G, & T_h g &= u, \\ \mathbf{S}: G &\rightarrow \mathbf{V} \subset G, & \mathbf{S}g &= \boldsymbol{\sigma}, \\ \mathbf{S}_h: G &\rightarrow \mathbf{V}_h \subset G, & \mathbf{S}_h g &= \boldsymbol{\sigma}_h. \end{aligned} \quad (4.8)$$

As a result, the operator form of the eigenvalue problems (3.3) and (4.1) can be equivalently converted as

$$\lambda T u = u, \mathbf{S}(\lambda u) = \boldsymbol{\sigma}, \tag{4.9}$$

$$\lambda_h T_h u_h = u_h, \mathbf{S}_h(\lambda_h u_h) = \boldsymbol{\sigma}_h. \tag{4.10}$$

Thus, solving the eigenvalue problem (3.3) for the eigenpair  $(\lambda, \boldsymbol{\sigma}, u)$  is equivalent to solving the eigenpair of the operator  $T$  for  $(\lambda^{-1}, u)$  and  $\boldsymbol{\sigma} = \mathbf{S}(\lambda u)$ . Similarly, solving the eigenvalue problem (4.1) for the eigenpair  $(\lambda_h, \boldsymbol{\sigma}_h, u_h)$  is equivalent to solving for the eigenpair of the operator  $T_h$  for  $(\lambda_h^{-1}, u_h)$  and  $\boldsymbol{\sigma}_h = \mathbf{S}_h(\lambda_h u_h)$ .

For the linear bounded operators  $T$  and  $\mathbf{S}$  defined in (4.8), for any  $g \in W$ , such that

$$\begin{cases} a(\mathbf{S}g, \boldsymbol{\Psi}) - b(\boldsymbol{\Psi}, Tg) + d(\boldsymbol{\Psi}, Tg) = 0, & \forall \boldsymbol{\Psi} \in \mathbf{V} \\ b(\mathbf{S}g, v) + e(Tg, v) = r(g, v), & \forall v \in W, \end{cases} \tag{4.11}$$

for this elliptic problem, the following regularity estimate holds [1]:

$$\|Tg\|_{1+\mu} \lesssim \|g\|_0, \tag{4.12}$$

where  $\mu = \pi/\omega - \varepsilon$ ,  $\omega < 2\pi$  being the maximum interior angle of  $\Omega$ .

For the discrete version of the linear bounded operators  $T_h$  and  $\mathbf{S}_h$  defined in (4.8), for any  $g \in W$ , such that

$$\begin{cases} a(\mathbf{S}_h g, \boldsymbol{\Psi}) - b(\boldsymbol{\Psi}, T_h g) + d(\boldsymbol{\Psi}, T_h g) = 0, & \forall \boldsymbol{\Psi} \in \mathbf{V}_h \\ b(\mathbf{S}_h g, v) + e(T_h g, v) = r(g, v), & \forall v \in W_h. \end{cases} \tag{4.13}$$

From the definitions of the operators (4.11), (4.13), and (4.6), we get

$$\Sigma_h T = T_h, \tag{4.14}$$

From (4.9), (4.10) and the projection definition (4.6), we obtain

$$\lambda_h \Sigma_h T u_h = u_h, \tag{4.15}$$

$$\lambda \Sigma_h T u = \Sigma_h u. \tag{4.16}$$

Since both  $T$  and  $T_h$  are self-adjoint operators, the eigenvalue  $\lambda$  in problem (3.3) is semi-simple, meaning its geometric multiplicity equals its algebraic multiplicity, and the slope is 1. Let  $M(\lambda)$  be the generalized eigenspace associated with the eigenvalue  $\lambda$ , and  $M_h(\lambda)$  be the direct sum of the generalized eigenspaces associated with  $\lambda_h$  in (4.1), where  $\lambda_h$  converges to  $\lambda$ .

when  $h$  is small enough, the mixed discretised source problem is well-posed and has a unique solution. According to theorem 4 in [1], we can obtain the following a priori estimates: For any  $f \in L^2(\Omega)$ , the following hold

$$\|\mathbf{S}f - \mathbf{S}_h f\|_0 \lesssim h^\beta \|Tf\|_{\beta+1}, \quad 1 \leq \beta \leq k+1, \tag{4.17}$$

$$\|div(\mathbf{S}f - \mathbf{S}_h f)\|_0 \lesssim h^\beta \|Tf\|_{\beta+2}, \quad 0 \leq \beta \leq k+1, \tag{4.18}$$

$$\|Tf - T_h f\|_0 \lesssim \begin{cases} h \|Tf\|_2, & k = 0, \\ h^\beta \|Tf\|_\beta, & k \geq 1 \text{ and } 2 \leq \beta \leq k+1. \end{cases} \tag{4.19}$$

By combining the Brezzi-Babuska theorem and the regularity of boundary value problems, if  $f \in M(\lambda)$ , then  $Tf = \lambda^{-1}f$ , and we obtain the following estimate:

$$\|(\mathbf{S} - \mathbf{S}_h)|_{M(\lambda)}\|_0 \lesssim h^\beta, \quad 1 \leq \beta \leq k+1, \tag{4.20}$$

$$\|div(\mathbf{S} - \mathbf{S}_h)|_{M(\lambda)}\|_0 \lesssim h^\beta, \quad 0 \leq \beta \leq k+1, \tag{4.21}$$

$$\|(T - T_h)|_{M(\lambda)}\|_0 \lesssim \begin{cases} h, & k = 0, \\ h^\beta, & k \geq 1 \text{ and } 2 \leq \beta \leq k+1. \end{cases} \tag{4.22}$$

Therefore, from (4.17) and (4.19), we derive the following convergence results

$$\|T - T_h\|_0 \rightarrow 0, \quad \text{if } h \rightarrow 0, \tag{4.23}$$

$$\|\mathbf{S} - \mathbf{S}_h\|_0 \rightarrow 0, \quad \text{if } h \rightarrow 0. \tag{4.24}$$

Equations (4.23) and (4.24) show the convergence of the eigenvalues and eigenfunctions. Consequently, by using the proof method in reference [14], we may draw the following conclusions.

**Lemma 4.1.** For each approximate eigenpair  $(\lambda_h, \boldsymbol{\sigma}_h, u_h)$ , there exists an exact eigenpair  $(\lambda, \boldsymbol{\sigma}, u)$  such that the following a priori error estimates hold

$$|\lambda - \lambda_h| \lesssim h^{2\alpha}, \tag{4.25}$$

$$\|\boldsymbol{\sigma} - \boldsymbol{\sigma}_h\|_V + \|u - u_h\|_0 \lesssim h^\alpha, \tag{4.26}$$

where  $\alpha = \min\{1, \mu\}$ ,  $\alpha = 1$  if  $\Omega$  is convex and  $\alpha = \mu$  for a nonconvex  $\Omega$ , due to regularity result (4.12).

## V. A POSTERIORI ERROR ANALYSIS

The purpose of this part is to determine posterior error estimates for the second-order elliptic eigenvalue issue and verify the reliability of the error indicators for eigenvalues and eigenfunctions in the mixed finite element method, as well as the effectiveness of the eigenfunction estimator.

### 5.1 Properties of The Mesh

Let us set some definitions before presenting posteriori error estimates. For  $\kappa \in \mathcal{T}_h$ , let  $\Gamma(\kappa)$  be the set of its edges, and let  $N(\kappa)$  be the set of its vertices . We define

$$\Gamma_h = \bigcup_{\kappa \in \mathcal{T}_h} \Gamma(\kappa) = \Gamma_h^0 \cup \Gamma_h^\partial, \quad \mathcal{N}_h = \bigcup_{\kappa \in \mathcal{T}_h} \mathcal{N}(\kappa).$$

For any edge  $E \in \Gamma_h$ , let  $\mathcal{N}(E)$  be the set of its vertices. Next, we define the sets listed below:

$$\begin{aligned} \omega_\kappa &= \bigcup_{\Gamma(\kappa) \cap \Gamma(\kappa') \neq \emptyset} \kappa', & \omega_E &= \bigcup_{E \in \Gamma(\kappa')} \kappa', & \omega_z &= \bigcup_{z \in \mathcal{N}(\kappa')} \kappa', \\ \tilde{\omega}_\kappa &= \bigcup_{\mathcal{N}(\kappa) \cap \mathcal{N}(\kappa') \neq \emptyset} \kappa', & \tilde{\omega}_E &= \bigcup_{\mathcal{N}(E) \cap \mathcal{N}(\kappa') \neq \emptyset} \kappa'. \end{aligned} \tag{5.1}$$

### 5.2 Superconvergence Analysis

In this section, to study the superconvergence of the eigenfunction interpolation  $Q_h u$  and the eigenfunction approximation  $u_h$  for the eigenvalue problem (3.1), we will focus on the superconvergence of the eigenfunction projection  $\Sigma_h u$  and the eigenfunction approximation  $u_h$ , based on the method in reference [10]. In this process, we will utilize the pertinent findings on the superconvergence of eigenfunction projection  $\Sigma_h u$  and eigenfunction interpolation  $Q_h u$  from Brezzi's study [8].

**Theorem 5.1.** Let  $(\lambda_h, \sigma_h, u_h)$  be the discrete eigenpair approximate solution corresponding to the eigenvalue problem (4.1), and  $(\Pi_h \sigma, \Sigma_h u)$  be the mixed finite element projection defined by (4.6). When the mesh size  $h$  is sufficiently small, the following superconvergence result holds:

$$\|\Sigma_h u - u_h\|_0 \lesssim h^{2\alpha}. \tag{5.2}$$

**Proof.** Define the function  $\mathcal{X}_h = \Sigma_h u - u_h - (\Sigma_h u - u_h, u)u$ , which  $\mathcal{X}_h$  consists of  $\Sigma_h u - u_h$  and  $(\Sigma_h u - u_h, u)u$ . Based on the definition  $\mathcal{X}_h$ , the following error estimate can be given

$$\|\Sigma_h u - u_h\|_0 \lesssim \|\mathcal{X}_h\|_0 + \|(\Sigma_h u - u_h, u)u\|_0, \tag{5.3}$$

therefore, to estimate the error of  $\|\Sigma_h u - u_h\|_0$ , we can decompose it into separate error estimates for  $\mathcal{X}_h$  and the term  $(\Sigma_h u - u_h, u)u$ .

(i) Estimate the error of  $\|(\Sigma_h u - u_h, u)u\|_0$ . According to the following equation

$$\begin{aligned} \|(\Sigma_h u - u_h, u)u\|_0 &\lesssim |(u, \Sigma_h u - u_h)| \\ &= |(u, \Sigma_h u - u)| + |(u, u - u_h)|, \end{aligned} \tag{5.4}$$

we only need to estimate the errors of  $|(u, \Sigma_h u - u)|$  and  $|(u, u - u_h)|$ .

First, estimate  $|(u, \Sigma_h u - u)|$ . According to (3.3), we have

$$\begin{aligned} \lambda(u, \Sigma_h u - u) &= \lambda r(u, \Sigma_h u - u) \\ &= -a(\sigma, \Psi) + b(\Psi, u) - d(\Psi, u) \\ &\quad + b(\sigma, \Sigma_h u - u) + e(u, \Sigma_h u - u), \forall \Psi \in \mathbf{V}, \end{aligned}$$

in the above equation, by taking  $\Psi = \Pi_h \sigma - \sigma$ , we get

$$\begin{aligned} \lambda(u, \Sigma_h u - u) &= -a(\sigma, \Pi_h \sigma - \sigma) + b(\Pi_h \sigma - \sigma, u) - d(\Pi_h \sigma - \sigma, u) \\ &\quad + b(\sigma, \Sigma_h u - u) + e(u, \Sigma_h u - u). \end{aligned} \tag{5.5}$$

In (4.6), by taking  $\Psi_h = \Pi_h \sigma$  and  $v_h = \Sigma_h u$ , we obtain

$$\begin{cases} a(\Pi_h \sigma - \sigma, \Pi_h \sigma) - b(\Pi_h \sigma, \Sigma_h u - u) + d(\Pi_h \sigma, \Sigma_h u - u) = 0, \\ -b(\Pi_h \sigma - \sigma, \Sigma_h u) - e(\Sigma_h u - u, \Sigma_h u) = 0 \end{cases}$$

substituting this into (5.5) gives

$$\begin{aligned} &\lambda(u, \Sigma_h u - u) \\ &= a(\Pi_h \sigma - \sigma, \Pi_h \sigma - \sigma) - b(\Pi_h \sigma - \sigma, \Sigma_h u - u) - b(\Pi_h \sigma - \sigma, \Sigma_h u - u) \\ &\quad - e(\Sigma_h u - u, \Sigma_h u - u) - d(\Pi_h \sigma - \sigma, u) + d(\Pi_h \sigma, \Sigma_h u - u). \end{aligned} \tag{5.6}$$

The following expression is deformed:

$$\begin{aligned} &-d(\Pi_h \sigma - \sigma, u) + d(\Pi_h \sigma, \Sigma_h u - u) \\ &= -d(\Pi_h \sigma - \sigma, u) + d(\Pi_h \sigma - \sigma + \sigma, \Sigma_h u - u) \\ &= -d(\Pi_h \sigma - \sigma, u) + d(\Pi_h \sigma - \sigma, \Sigma_h u) - d(\Pi_h \sigma - \sigma, u) + d(\sigma, \Sigma_h u - u) \\ &= d(\Pi_h \sigma - \sigma, \Sigma_h u - u) - d(\Pi_h \sigma, u) + d(\sigma, \Sigma_h u), \end{aligned}$$

Since  $\|\Pi_h \sigma\|_0 \lesssim \|\sigma\|_0$  and  $\|\Sigma_h u\|_0 \lesssim \|u\|_0$  are infinitesimals, substituting the above expressions into (5.6) and combining with (4.7), we obtain

$$|(u, \Sigma_h u - u)| \lesssim h^{2\alpha}. \tag{5.7}$$

Afterward, we estimate the error of  $|(u, u - u_h)|$ . Based on (4.17), we get

$$\begin{aligned} |(u, u - u_h)| &= \left| \frac{1}{2}(u, u) - (u, u_h) + \frac{1}{2}(u, u) \right| \\ &= \left| \frac{1}{2}(u, u) - \frac{1}{2}(u, u_h) - \frac{1}{2}(u, u_h) + \frac{1}{2}(u_h, u_h) \right| \\ &= \left| \frac{1}{2}(u, u - u_h) - \frac{1}{2}(u_h, u - u_h) \right| \\ &= \frac{1}{2}|(u - u_h, u - u_h)| \\ &\lesssim h^{2\alpha}. \end{aligned} \tag{5.8}$$

Thus, substituting (5.7) and (5.8) into (5.4), we easily get

$$\|(\Sigma_h u - u_h, u)\|_0 \lesssim h^{2\alpha}. \tag{5.9}$$

(ii) Estimation of the error in  $\|\mathcal{X}_h\|_0$ . Since  $(u, u) = 1$ , we have  $(\mathcal{X}_h, u) = 0$ , and thus

$$\|\mathcal{X}_h\|_0 \lesssim \|(I - \lambda T)\mathcal{X}_h\|_0 = \|(I - \lambda T)(\Sigma_h u - u_h)\|_0. \tag{5.10}$$

From (4.15) and (4.16), we have

$$\begin{aligned} & (I - \lambda T)(\Sigma_h u - u_h) \\ &= -\lambda T(\Sigma_h u - u_h) + (\Sigma_h u - u_h) \\ &= (\lambda_h \Sigma_h T - \lambda T - \lambda_h \Sigma_h T)(\Sigma_h u - u_h) + (\Sigma_h u - u_h) \\ &= -\lambda_h \Sigma_h T(\Sigma_h u - u_h) + (\Sigma_h u - u_h) + (\lambda_h \Sigma_h T - \lambda T)(\Sigma_h u - u_h) \\ &= -\lambda_h \Sigma_h T(u - u_h) + (\Sigma_h u - u_h) - \lambda_h \Sigma_h T(\Sigma_h u - u) + (\lambda_h \Sigma_h T - \lambda T)(\Sigma_h u - u_h) \\ &= (\lambda - \lambda_h)\Sigma_h T u - \lambda_h \Sigma_h T(\Sigma_h u - u) + (\lambda_h \Sigma_h T - \lambda T)(\Sigma_h u - u_h). \end{aligned} \tag{5.11}$$

Using (5.10) and (5.11), we can obtain

$$\|\mathcal{X}_h\|_0 \lesssim \|(\lambda_h \Sigma_h T - \lambda T)(\Sigma_h u - u_h)\|_0 + |\lambda_h - \lambda| \cdot \|\Sigma_h T u\|_0 + \lambda_h \|\Sigma_h T(\Sigma_h u - u)\|_0, \tag{5.12}$$

also, the first equation of (5.12) can be rewritten as

$$\begin{aligned} & (\lambda_h \Sigma_h T - \lambda T) \cdot (\Sigma_h u - u_h) \\ &= (\lambda_h \Sigma_h T - \lambda \Sigma_h T + \lambda \Sigma_h T - \lambda T) \cdot (\Sigma_h u - u_h) \\ &= (\lambda_h - \lambda) \cdot \Sigma_h T(\Sigma_h u - u_h) + \lambda(\Sigma_h - I)T \cdot (\Sigma_h u - u_h) \\ &\lesssim |\lambda_h - \lambda| \cdot \|\Sigma_h T(\Sigma_h u - u_h)\|_0 + \lambda \|(\Sigma_h - I)T(\Sigma_h u - u_h)\|_0. \end{aligned}$$

Therefore, using (4.7), (4.12), and (4.25), we have

$$\begin{aligned} \|\mathcal{X}_h\|_0 &\lesssim h^{2\alpha} \|\Sigma_h T(\Sigma_h u - u_h)\|_0 + \lambda h^\alpha \|T(\Sigma_h u - u_h)\|_2 \\ &\quad + h^{2\alpha} \|Tu\|_{1+\mu} + \lambda_h \|\Sigma_h T(\Sigma_h u - u)\|_0 \\ &\lesssim h^{2\alpha} \|\Sigma_h u - u_h\|_0 + \lambda h^\alpha \|\Sigma_h u - u_h\|_0 \\ &\quad + h^{2\alpha} \|u\|_0 + \lambda_h \|\Sigma_h T(\Sigma_h u - u)\|_0 \\ &\lesssim h^{2\alpha} \|u\|_0 + \lambda h^\alpha \|\Sigma_h u - u_h\|_0 + \lambda_h \|\Sigma_h T(\Sigma_h u - u)\|_0. \end{aligned} \tag{5.13}$$

In (5.13), we also need to estimate the third term  $\|\Sigma_h T(\Sigma_h u - u)\|_0$  of  $\|\mathcal{X}_h\|_0$ . First, we define a function  $g_h \in W_h$  such that  $\|g_h\|_0 = 1$ , and it satisfies the condition

$$r(g_h, \Sigma_h T(\Sigma_h u - u)) = \|\Sigma_h T(\Sigma_h u - u)\|_0.$$

Next, we define an auxiliary equation: Find  $(\boldsymbol{\eta}_h, \xi_h) \in \mathbf{V}_h \times W_h$ , such that

$$\begin{cases} a(\boldsymbol{\Psi}_h, \boldsymbol{\eta}_h) - b(\boldsymbol{\Psi}_h, \xi_h) + d(\boldsymbol{\eta}_h, v_h) = 0, & \forall \boldsymbol{\Psi}_h \in \mathbf{V}_h \\ b(\boldsymbol{\eta}_h, v_h) + e(v_h, \xi_h) = r(g_h, v_h), & \forall v_h \in W_h \end{cases} \tag{5.14}$$

Based on the Babuška–Brezzi condition of the mixed finite element space  $\mathbf{V}_h \times W_h$ , the following relation holds

$$\begin{aligned} \|\boldsymbol{\eta}_h\|_{\mathbf{V}} + \|\xi_h\|_0 &\lesssim \sup_{0 \neq (\boldsymbol{\Psi}_h, v_h) \in \mathbf{V}_h \times W_h} \frac{a(\boldsymbol{\Psi}_h, \boldsymbol{\eta}_h) - b(\boldsymbol{\Psi}_h, \xi_h)}{\|\boldsymbol{\Psi}_h\|_{\mathbf{V}} + \|v_h\|_0} \\ &\quad + \sup_{0 \neq (\boldsymbol{\Psi}_h, v_h) \in \mathbf{V}_h \times W_h} \frac{d(\boldsymbol{\eta}_h, v_h) + b(\boldsymbol{\eta}_h, v_h) + e(v_h, \xi_h)}{\|\boldsymbol{\Psi}_h\|_{\mathbf{V}} + \|v_h\|_0} \\ &\lesssim \sup_{0 \neq (\boldsymbol{\Psi}_h, v_h) \in \mathbf{V}_h \times W_h} \frac{r(g_h, v_h)}{\|\boldsymbol{\Psi}_h\|_{\mathbf{V}} + \|v_h\|_0} \\ &\lesssim \|g_h\|_0. \end{aligned} \tag{5.15}$$

Choosing  $(\boldsymbol{\Psi}_h, v_h) = (\boldsymbol{\Pi}_h \mathbf{S}(\Sigma_h u - u), \Sigma_h T(\Sigma_h u - u))$  in (5.14) and from (4.6), (4.11), and (4.13), we have

$$\begin{aligned} & -r(g_h, \Sigma_h T(\Sigma_h u - u)) \\ &= a(\boldsymbol{\Pi}_h \mathbf{S}(\Sigma_h u - u), \boldsymbol{\eta}_h) - b(\boldsymbol{\eta}_h, \Sigma_h T(\Sigma_h u - u)) \\ &\quad + d(\boldsymbol{\eta}_h, \Sigma_h T(\Sigma_h u - u)) - b(\boldsymbol{\Pi}_h \mathbf{S}(\Sigma_h u - u), \xi_h) - e(\Sigma_h T(\Sigma_h u - u), \xi_h) \\ &= a(\mathbf{S}(\Sigma_h u - u), \boldsymbol{\eta}_h) - b(\boldsymbol{\eta}_h, T(\Sigma_h u - u)) + d(\boldsymbol{\eta}_h, T(\Sigma_h u - u)) \\ &\quad - b(\mathbf{S}(\Sigma_h u - u), \xi_h) - e(T(\Sigma_h u - u), \xi_h) \\ &= -r(\Sigma_h u - u, \xi_h). \end{aligned} \tag{5.16}$$

Furthermore, based on the results in reference [8], Brezzi analyzed the superconvergence property of the characteristic function projection  $\Sigma_h u$  and the characteristic function interpolation  $Q_h u$ , i.e.

$$\|\Sigma_h u - Q_h u\|_0 \lesssim h^{2\alpha}. \tag{5.17}$$

From (5.15) and (5.17), we obtain the following estimate

$$\begin{aligned} r(\Sigma_h u - u, \xi_h) &= r(\Sigma_h u - Q_h u, \xi_h) + r(Q_h u - u, \xi_h) \\ &\lesssim h^{2\alpha} \|\xi_h\|_0 + \|Q_h u - u\|_0 \cdot \|\xi_h\|_0 \\ &\lesssim h^{2\alpha} \|g_h\|_0. \end{aligned} \tag{5.18}$$

Combining (5.16), (5.18), and the definition of  $g_h$ , we obtain the estimate  $\|\Sigma_h T(\Sigma_h u - u)\|_0 \lesssim h^{2\alpha}$ .

Thus, we have

$$\|\mathcal{X}_h\|_0 \lesssim h^{2\alpha} \|u\|_0 + \lambda h^\alpha \|\Sigma_h u - u_h\|_0 + \lambda_h h^{2\alpha}$$

$$\lesssim h^{2\alpha} + \lambda h^\alpha \|\Sigma_h u - u_h\|_0. \tag{5.19}$$

Finally, combining (i) and (ii) leads to

$$\|\Sigma_h u - u_h\|_0 \lesssim h^{2\alpha} + \lambda h \|\Sigma_h u - u_h\|_0, \tag{5.20}$$

It means when  $h$  is small enough, we have

$$\|\Sigma_h u - u_h\|_0 \lesssim h^{2\alpha} \tag{5.21}$$

The proof is complete.

**Corollary 5.1.** For the eigenfunction approximation  $u_h$  of the eigenvalue problem (3.3) and the interpolation  $Q_h u$  of the exact eigenfunction, when the mesh size  $h$  is small enough, the following superconvergence result holds

$$\|u_h - Q_h u\|_0 \lesssim h^{2\alpha}. \tag{5.22}$$

**Proof.** From (5.2) and (5.17), we have

$$\|u_h - Q_h u\|_0 \leq \|u_h - \Sigma_h u\|_0 + \|\Sigma_h u - Q_h u\|_0 \lesssim h^{2\alpha}.$$

Thus, the proof is complete.

### 5.3 Postprocessing Technique

Based on the superconvergence result (5.22), using a suitable post-processing operator to  $u_h$  can get an eigenfunction approximation with superconvergence properties. This postprocessing technique is highly effective in numerical computations, as it can significantly improve the accuracy of the solution without increasing the computational costs.

**Lemma 5.2.** (see Theorem 3.1 in [9]) There exists the following estimate for the eigenvalue approximation  $\lambda_h$ ,

$$|\lambda - \lambda_h|^{\frac{1}{2}} \lesssim \|\sigma - \sigma_h\|_V + \|u - u_h\|_0. \tag{5.23}$$

**Proof.** To extend the eigenvalue error, we now introduce the Rayleigh quotient (see [10]). Assume  $(\lambda, \sigma, u)$  is the true solution of the eigenvalue problem (3.3),  $\varphi \in \mathbf{V}$  and  $0 \neq s \in W$  satisfy

$$a(\varphi, \varphi) - b(\varphi, s) + d(\varphi, s) = 0. \tag{5.24}$$

Let us define the Rayleigh quotient for the eigenvalue  $\hat{\lambda}$  as

$$\hat{\lambda} = \frac{a(\varphi, \varphi) + d(\varphi, s) + e(s, s)}{r(s, s)}, \tag{5.25}$$

then, we rewrite  $a(\varphi, \varphi)$ ,  $d(\varphi, s)$ , and  $e(s, s)$  in the following forms

$$\begin{aligned} a(\varphi, \varphi) &= a(\varphi - \sigma + \sigma, \varphi - \sigma + \sigma) \\ &= a(\varphi - \sigma, \varphi - \sigma) + 2a(\varphi, \sigma) - a(\sigma, \sigma), \\ d(\varphi, s) &= d(\varphi - \sigma + \sigma, s - u + u) \\ &= d(\varphi - \sigma, s - u) - d(\sigma, u - s) + d(\varphi, u), \\ e(s, s) &= e(s - u + u, s - u + u) \\ &= e(s - u, s - u) + 2e(s, u) - e(u, u). \end{aligned}$$

Inserting these expressions into (5.25), according to (3.4), we get

$$\begin{aligned} \hat{\lambda} - \lambda &= \frac{a(\varphi, \varphi) + d(\varphi, s) + e(s, s) - \lambda r(s, s)}{r(s, s)} \\ &= \frac{a(\varphi - \sigma, \varphi - \sigma) + d(\varphi - \sigma, s - u) + e(s - u, s - u)}{r(s, s)} \\ &\quad + \frac{2[a(\varphi, \sigma) + e(s, u)] + d(\sigma, s) + d(\varphi, u) - \lambda r(u, u) + \lambda r(s, s)}{r(s, s)}. \end{aligned} \tag{5.26}$$

From (3.3) and (5.24), we obtain

$$\begin{aligned} &2[a(\varphi, \sigma) + e(s, u)] + d(\sigma, s) + d(\varphi, u) - \lambda r(u, u) - \lambda r(s, s) \\ &= 2[a(\varphi, \sigma) + e(s, u)] + d(\sigma, s) + d(\varphi, u) - \lambda r(s - u, s - u) - 2\lambda r(s, u) \\ &= 2[a(\varphi, \sigma) + e(s, u)] + d(\sigma, s) + d(\varphi, u) - 2[b(\sigma, s) + e(s, u)] - \lambda r(s - u, s - u) \\ &= 2[a(\varphi, \sigma) - b(\sigma, s)] + d(\sigma, s) + d(\varphi, u) - \lambda r(s - u, s - u) \\ &= 2[a(\varphi, \sigma) - b(\sigma, s) - a(\varphi, \varphi) + b(\varphi, s) - d(\varphi, s)] + d(\sigma, s) + d(\varphi, u) - \lambda r(s - u, s - u) \\ &= 2[a(\varphi, \sigma - \varphi) - b(\sigma - \varphi, s)] + d(\sigma - \varphi, s) - d(\varphi, s - u) - \lambda r(s - u, s - u) \\ &= 2[a(\varphi, \sigma - \varphi) - b(\sigma - \varphi, s) - a(\sigma, \sigma) + b(\sigma, u) - d(\sigma, u) + a(\sigma, \varphi) - b(\varphi, u) + d(\varphi, u)] \\ &\quad + d(\sigma - \varphi, s) - d(\varphi, s - u) - \lambda r(s - u, s - u) \\ &= 2[a(\varphi - \sigma, \sigma - \varphi) - b(\sigma - \varphi, s - u)] + d(\sigma - \varphi, s - u) \\ &\quad - d(\varphi, s - u) - d(\sigma - \varphi, u) - \lambda r(s - u, s - u) \end{aligned}$$

Finally, we obtain

$$\begin{aligned} \hat{\lambda} - \lambda &= \frac{2b(\varphi - \sigma, s - u) + e(s - u, s - u)}{r(s, s)} \\ &\quad - \frac{a(\varphi - \sigma, \varphi - \sigma) + d(\varphi, s - u) + d(\sigma - \varphi, u) + \lambda r(s - u, s - u)}{r(s, s)}. \end{aligned} \tag{5.27}$$

In conclusion, combining (5.27), (3.4), and (4.2), we can obtain the estimate for  $\lambda - \lambda_h$ , as shown in (5.23).

A superconvergent approximation of the eigenfunction can be obtained by combining the superconvergence result (5.22) with an appropriate interpolating postprocessing method. The post-processing operator of this type will be introduced in detail next.

We define a piecewise linear finite element space  $U_h$  as follows

$$U_h = \{v \in H^1(\Omega) : v|_{\kappa} \in P_1(\kappa), \forall \kappa \in \mathcal{T}_h\}. \tag{5.28}$$

For each vertex  $z$  in the mesh  $\mathcal{T}_h$ , we define the region  $\omega_z$  associated with this vertex, which consists of all elements adjacent to the vertex  $z$ . Next, we introduce a post-processing operator  $\Lambda_h: W \rightarrow U_h$ , which aims to improve the solution accuracy by fitting a piecewise linear function at the vertices. The following is the precise post-processing technique:

$$\Lambda_h v(z) = \sum_{\kappa \in \omega_z} \frac{\int_{\kappa} v dx}{|\omega_z|}, \tag{5.29}$$

where  $\Lambda_h v(z)$  represents the post-processed value at the vertex  $z \in \omega_z$ ;  $\int_{\kappa} v dx$  is the integral of function  $v$  over element  $\kappa$ ; and  $|\omega_z|$  is the area of the region  $\omega_z$  which is the total area of all elements containing vertex  $z$ .

Note that  $\Lambda_h v(z)$  is obtained by averaging the integrals of all elements sharing that vertex.

Let's review some important properties of  $\Lambda_h$  (see [11], Lemma 4.1).

**Lemma 5.3.** The operator  $\Lambda_h$  defined above satisfies the following:

- (i) For  $v \in H^{1+\alpha}(\kappa)$  and  $\kappa \in \mathcal{T}_h$ , we have  $\|\Lambda_h v - v\|_{0,\kappa} \lesssim h_{\kappa}^{1+\alpha} \|v\|_{2,\tilde{\omega}_{\kappa}}$ ;
- (ii) For any  $v \in W$ , we have  $\Lambda_h Q_h v = \Lambda_h v$ ;
- (iii) For any  $v \in W$ , we have  $\|\Lambda_h v\|_0 \lesssim \|v\|_0$ .

We may determine the superconvergence result of  $\Lambda_h$  based on Lemma 5.3.

**Lemma 5.4.** (Superconvergence) When  $h$  small enough, there holds

$$\|\Lambda_h v_h - v\|_0 \lesssim h^{2\alpha}. \tag{5.30}$$

**Proof.** Based on (5.22) and Lemma 5.3, we have

$$\begin{aligned} \|\Lambda_h v_h - v\|_0 &\lesssim \|\Lambda_h v_h - \Lambda_h Q_h v + \Lambda_h Q_h v - \Lambda_h v + \Lambda_h v - v\|_0 \\ &\lesssim \|\Lambda_h v_h - \Lambda_h Q_h v\|_0 + \|\Lambda_h Q_h v - \Lambda_h v\|_0 + \|\Lambda_h v - v\|_0 \\ &\lesssim \|v_h - Q_h v\|_0 + \|\Lambda_h v - v\|_0 \\ &\lesssim h^{2\alpha}. \end{aligned}$$

### 5.4 Technical Tools

To perform the analysis, we recall two key properties that are needed. First, let us consider the operator  $O_h: H^1(\Omega) \rightarrow M_I$ , where

$$M_I = \{p \in C(\bar{\Omega}) : p|_{\kappa} \in P_1(\kappa), \forall \kappa \in \mathcal{T}_h\},$$

is the Clément interpolant of degree  $k = 1$  (see [12]).

We now establish the following lemma, which states the local approximation properties of  $O_h$ .

**Lemma 5.5.** For all  $p \in H^1(\Omega)$ , there holds

$$\|p - O_h p\|_{0,\kappa} \lesssim h_{\kappa} \|p\|_{1,\tilde{\omega}_{\kappa}}, \forall \kappa \in \mathcal{T}_h \tag{5.31}$$

$$\|p - O_h p\|_{0,E} \lesssim h_E^{1/2} \|p\|_{1,\tilde{\omega}_E}, \forall E \in \Gamma_h \tag{5.32}$$

Secondly, the following Helmholtz decomposition holds.

**Lemma 5.6.** For each  $\sigma \in H(\text{div}; \Omega)$  there exist  $\phi \in H_0^1(\Omega)$  and  $p \in H^1(\Omega)$  such that  $\int_{\Omega} p dx = 0$ , and they satisfy the equation

$$\sigma = \nabla \phi + \text{curl} p, \text{ in } \Omega, \tag{5.33}$$

and the following norm relation holds  $\|\sigma\|_0 = (\|\nabla \phi\|_0^2 + \|\text{curl} p\|_0^2)^{\frac{1}{2}}$ .

### 5.5 The Local And Global Error Indicators

Based on the previous superconvergence results and the related theory of post-processing operators, we next derive the local error estimator and the global error estimator, and analyze their reliability and effectiveness in eigenvalue and eigenfunction estimation.

Let  $(\lambda_h, \sigma_h, u_h)$  be the eigenpair of (4.1). For each edge  $E \in \Gamma_h$ , we define the surface residual as follows

$$J_F = \begin{cases} [(\sigma_h - \mathbf{b}u_h) \cdot \mathbf{t}], & E \in \Gamma_h^0 \\ (\sigma_h - \mathbf{b}u_h) \cdot \mathbf{t}, & E \in \Gamma_h^{\partial}, \end{cases}$$

where  $\mathbf{t}$  denotes the tangential vector in the clockwise direction on edge  $E$ .

Let us present the indicator for the reduced discrete eigenvalue problem

$$\eta_{\kappa}^2 = h_{\kappa}^2 \|rot(\sigma_h - \mathbf{b}u_h)\|_{0,\kappa}^2 + \|\Lambda_h u_h - u_h\|_{0,\kappa}^2 + \|c - Q_h c\|_{0,\kappa}^2 + \sum_{E \in \Gamma(\kappa)} h_E \|J_F\|_{0,E}^2, \tag{5.34}$$

and the global estimator is defined by



$$\eta = \left( \sum_{\kappa \in \mathcal{T}_h} \eta_\kappa^2 \right)^{\frac{1}{2}}. \tag{5.35}$$

### 5.6 Reliability Of Error Estimators For Eigenfunctions And Eigenvalue

The goal of this section is to derive an upper bound for (4.22). Let us begin with the following result.

**Lemma 5.7.** For the approximation of the eigenfunctions  $(\sigma_h, u_h)$ , we have the following estimate

$$\|\sigma - \sigma_h\|_V + \|u - u_h\|_0 \lesssim \|c - Q_h c\|_0 + \|A_h u_h - u_h\|_0 + \|A_h u_h - u\|_0 + |\lambda - \lambda_h| + \|\mathbf{curl} p\|_0 \tag{5.36}$$

where  $\|A_h u_h - u\|_0 + |\lambda - \lambda_h|$  are the higher-order terms.

**Proof.** (i) First, we estimate the error for the scalar variable approximation  $u_h$ ,

$$\begin{aligned} \|u - u_h\|_0 &\leq \|u - A_h u_h + A_h u_h - u_h\|_0 \\ &\leq \|A_h u_h - u_h\|_0 + \|u - A_h u_h\|_0 \\ &\leq \|A_h u_h - u_h\|_0 + \|A_h u_h - u\|_0 + |\lambda - \lambda_h|, \end{aligned} \tag{5.37}$$

the scalar function is estimated by (5.30) and (5.37).

(ii) Now, we consider the estimation of the error  $\|\sigma - \sigma_h\|_V$ . Since

$$\|\sigma - \sigma_h\|_V = (\|\sigma - \sigma_h\|_0^2 + \|\mathit{div}(\sigma - \sigma_h)\|_0^2)^{\frac{1}{2}},$$

the values for  $\|\sigma - \sigma_h\|_0$  and  $\|\mathit{div}(\sigma - \sigma_h)\|_0$  must be estimated independently.

First, we consider the estimation of  $\|\mathit{div}(\sigma - \sigma_h)\|_0$ . Using the first equation in (3.2) and the second equation in (4.1), we get

$$\begin{aligned} \mathit{div} \sigma &= cu - \lambda u, \\ \mathit{div} \sigma_h &= cu_h - \lambda_h u_h = Q_h cu_h - \lambda_h Q_h u_h. \end{aligned}$$

Thus,

$$\begin{aligned} \mathit{div}(\sigma - \sigma_h) &= (cu - Q_h cu_h) - \lambda u + \lambda_h Q_h u_h \\ &= (cu - Q_h cu + Q_h cu - Q_h cu_h) - \lambda u + (\lambda Q_h u - \lambda Q_h u + \lambda_h Q_h u_h - \lambda_h Q_h u + \lambda_h Q_h u) \\ &= (c - Q_h c)u + Q_h c(u - u_h) - \lambda(I - Q_h)u - (\lambda - \lambda_h)Q_h u - \lambda_h Q_h(u - u_h). \end{aligned}$$

From part (i), we can infer the following inequality

$$\begin{aligned} \|\mathit{div}(\sigma - \sigma_h)\|_0 &\lesssim \|c - Q_h c\|_0 + \|u - u_h\|_0 + |\lambda - \lambda_h| + \lambda_h \|u - u_h\|_0 \\ &\lesssim \|c - Q_h c\|_0 + \|A_h u_h - u_h\|_0 + \|A_h u_h - u\|_0 + |\lambda - \lambda_h|, \end{aligned} \tag{5.38}$$

The next step is to estimate the  $L^2$  norm of the vector variable  $\sigma - \sigma_h$ . Lemma 5.6 states that the error can be decomposed as follows

$$\sigma - \sigma_h = \nabla \phi + \mathbf{curl} p. \tag{5.39}$$

where  $\phi \in H_0^1(\Omega)$  and  $p \in H^1(\Omega)$ , with  $\int_\Omega p dx = 0$ .

To conclude, we need to estimate  $\|\nabla \phi\|_0$ . Using (5.39) and Green's formula, we get

$$\begin{aligned} \|\nabla \phi\|_0^2 &= \int_\Omega \nabla \phi \cdot \nabla \phi dx \\ &= \int_\Omega (\sigma - \sigma_h) \cdot \nabla \phi dx - \int_\Omega \mathbf{curl} p \cdot \nabla \phi dx \\ &= - \int_\Omega \mathit{div}(\sigma - \sigma_h) \cdot \phi dx - \int_\Omega \mathbf{curl} p \cdot \nabla \phi dx \\ &\lesssim \|\mathit{div}(\sigma - \sigma_h)\|_0 \|\phi\|_0 + \|\mathbf{curl} p\|_0 \|\nabla \phi\|_0 \end{aligned} \tag{5.40}$$

Since  $\phi \in H_0^1(\Omega)$ , the following inequality holds

$$\|\nabla \phi\|_0 \lesssim \|\mathit{div}(\sigma - \sigma_h)\|_0 + \|\mathbf{curl} p\|_0. \tag{5.41}$$

Consequently, combining (5.37) - (5.39) and (5.41), we obtain

$$\begin{aligned} \|\sigma - \sigma_h\|_0 &\leq \|\nabla \phi\|_0 + \|\mathbf{curl} p\|_0 \\ &\lesssim \|\mathit{div}(\sigma - \sigma_h)\|_0 + \|\mathbf{curl} p\|_0 \\ &\lesssim \|c - Q_h c\|_0 + \|A_h u_h - u_h\|_0 + \|A_h u_h - u\|_0 + |\lambda - \lambda_h| + \|\mathbf{curl} p\|_0. \end{aligned}$$

Thus, we get the final result

$$\|\sigma - \sigma_h\|_V \lesssim \|c - Q_h c\|_0 + \|A_h u_h - u_h\|_0 + \|A_h u_h - u\|_0 + |\lambda - \lambda_h| + \|\mathbf{curl} p\|_0.$$

combining (i) and (ii), we obtain the result of (5.36).

**Theorem 5.2.** For  $h$  small enough, there holds

$$\|\sigma - \sigma_h\|_V + \|u - u_h\|_0 \lesssim \eta + \|A_h u_h - u\|_0 + |\lambda - \lambda_h|, \tag{5.42}$$

and

$$|\lambda - \lambda_h|^{1/2} \lesssim \eta + \|A_h u_h - u\|_0 + |\lambda - \lambda_h|. \tag{5.43}$$

where  $\|A_h u_h - u\|_0 + |\lambda - \lambda_h|$  is the higher order term.

**Proof.** To prove (5.42) and (5.43), it suffices to estimate  $\|\mathbf{curl} p\|_0$ . Since  $\mathbf{curl} p = (\sigma - \sigma_h) - \nabla \phi$ , we have

$$\begin{aligned} \|\mathbf{curl}p\|_0^2 &= \int_{\Omega} \mathbf{curl}p \cdot \mathbf{curl}p dx \\ &= \int_{\Omega} (\boldsymbol{\sigma} - \boldsymbol{\sigma}_h) \cdot \mathbf{curl}p dx - \int_{\Omega} \nabla\phi \cdot \mathbf{curl}p dx, \end{aligned}$$

by using Green's theorem to handle  $-\int_{\Omega} \nabla\phi \cdot \mathbf{curl}p dx$ , we get

$$-\int_{\Omega} \nabla\phi \cdot \mathbf{curl}p dx = \int_{\Omega} \phi \cdot \operatorname{div}\mathbf{curl}p dx - \int_{\partial\Omega} \phi \cdot \mathbf{curl}p \cdot \mathbf{n} ds.$$

Therefore, we obtain

$$\|\mathbf{curl}p\|_0^2 = \int_{\Omega} (\boldsymbol{\sigma} - \boldsymbol{\sigma}_h) \cdot \mathbf{curl}p dx. \tag{5.44}$$

Since  $\boldsymbol{\sigma} = \nabla u + \mathbf{b}(x)u$ , applying Green's theorem to  $\int_{\Omega} \boldsymbol{\sigma} \cdot \mathbf{curl}p dx$ , we get

$$\int_{\Omega} \boldsymbol{\sigma} \cdot \mathbf{curl}p dx = \int_{\Omega} \mathbf{b}u \cdot \mathbf{curl}p dx. \tag{5.45}$$

By Lemma 5.5,  $O_h p$  is the continuous piecewise linear approximation of  $p$ , so  $\mathbf{curl}O_h p \in \mathbf{V}_h$  and  $\operatorname{div}\mathbf{curl}O_h p = 0$ . From the first equation of (4.1), we get

$$\int_{\Omega} \boldsymbol{\sigma}_h \cdot \mathbf{curl}O_h p dx = \int_{\Omega} \mathbf{b}u_h \cdot \mathbf{curl}O_h p dx. \tag{5.46}$$

Substituting (5.45) and (5.46) into (5.44), we obtain

$$\begin{aligned} &\|\mathbf{curl}p\|_0^2 \\ &= -\int_{\Omega} \boldsymbol{\sigma}_h \cdot \mathbf{curl}p dx + \int_{\Omega} \mathbf{b}u \cdot \mathbf{curl}p dx \\ &= -\int_{\Omega} \boldsymbol{\sigma}_h \cdot \mathbf{curl}p dx + \int_{\Omega} \mathbf{b}u \cdot \mathbf{curl}p dx + \int_{\Omega} \boldsymbol{\sigma}_h \cdot \mathbf{curl}O_h p dx - \int_{\Omega} \mathbf{b}(u_h + u - u) \cdot \mathbf{curl}O_h p dx \\ &= -\int_{\Omega} \boldsymbol{\sigma}_h \cdot \mathbf{curl}(p - O_h p) dx + \int_{\Omega} \boldsymbol{\sigma}_h \cdot \mathbf{curl}(p - O_h p) dx + \int_{\Omega} (\mathbf{b}u - \mathbf{b}u_h) \cdot \mathbf{curl}O_h p dx \\ &= -\int_{\Omega} \boldsymbol{\sigma}_h \cdot \mathbf{curl}(p - O_h p) dx + \int_{\Omega} \mathbf{b}u_h \cdot \mathbf{curl}(p - O_h p) dx - \int_{\Omega} \mathbf{b}u_h \cdot \mathbf{curl}(p - O_h p) dx \\ &\quad + \int_{\Omega} \mathbf{b}u \cdot \mathbf{curl}(p - O_h p) dx + \int_{\Omega} (\mathbf{b}u - \mathbf{b}u_h) \cdot \mathbf{curl}O_h p dx \\ &= -\int_{\Omega} (\boldsymbol{\sigma}_h - \mathbf{b}u_h) \cdot \mathbf{curl}(p - O_h p) dx + \int_{\Omega} (\mathbf{b}u - \mathbf{b}u_h) \cdot \mathbf{curl}(p - O_h p) dx + \int_{\Omega} (\mathbf{b}u - \mathbf{b}u_h) \cdot \mathbf{curl}O_h p dx \\ &= -\int_{\Omega} (\boldsymbol{\sigma}_h - \mathbf{b}u_h) \cdot \mathbf{curl}(p - O_h p) dx + \int_{\Omega} (\mathbf{b}u - \mathbf{b}u_h) \cdot \mathbf{curl}(p - O_h p) dx \\ &\quad + \int_{\Omega} (\mathbf{b}u - \mathbf{b}u_h) \cdot \mathbf{curl}(O_h p - p + p) dx \\ &= -\int_{\Omega} (\boldsymbol{\sigma}_h - \mathbf{b}u_h) \cdot \mathbf{curl}(p - O_h p) dx + \int_{\Omega} \mathbf{b}(u - u_h) \cdot \mathbf{curl}p dx. \end{aligned}$$

Moreover, we have

$$\begin{aligned} &-\int_{\Omega} (\boldsymbol{\sigma}_h - \mathbf{b}u_h) \cdot \mathbf{curl}(p - O_h p) dx \\ &= -\sum_{\kappa \in \mathcal{T}_h} \int_{\kappa} \operatorname{rot}(\boldsymbol{\sigma}_h - \mathbf{b}u_h)(p - O_h p) dx + \sum_{\kappa \in \mathcal{T}_h} \int_{\partial\kappa} (\boldsymbol{\sigma}_h - \mathbf{b}u_h) \cdot \mathbf{t}(p - O_h p) ds \\ &= -\sum_{\kappa \in \mathcal{T}_h} \int_{\kappa} \operatorname{rot}(\boldsymbol{\sigma}_h - \mathbf{b}u_h)(p - O_h p) dx + \sum_{\kappa \in \mathcal{T}_h} \sum_{E \in \Gamma(\kappa)} \int_E J_F \cdot (p - O_h p) ds, \end{aligned}$$

and

$$\int_{\Omega} \mathbf{b}(u - u_h) \cdot \mathbf{curl}p dx = \sum_{\kappa \in \mathcal{T}_h} \int_{\kappa} \mathbf{b}(u - u_h) \cdot \mathbf{curl}p dx,$$

expanding further and integrating the earlier findings, we obtain

$$\begin{aligned} \|\mathbf{curl}p\|_0^2 &\lesssim \sum_{\kappa \in \mathcal{T}_h} \|\operatorname{rot}(\boldsymbol{\sigma}_h - \mathbf{b}u_h)\|_{0,\kappa} \cdot \|p - O_h p\|_{0,\kappa} \\ &\quad + \sum_{\kappa \in \mathcal{T}_h} \sum_{E \in \Gamma(\kappa)} \|J_F\|_{0,E} \cdot \|p - O_h p\|_{0,E} + \sum_{\kappa \in \mathcal{T}_h} \|u - u_h\|_{0,\kappa} \cdot \|\mathbf{curl}p\|_{0,\kappa}, \end{aligned}$$

applying the Schwarz inequality, (5.31), (5.32), and (5.37), we obtain

$$\begin{aligned} \|\mathbf{curl}p\|_0 &\lesssim \sum_{\kappa \in \mathcal{T}_h} \left\{ h_\kappa^2 \|\mathbf{rot}(\boldsymbol{\sigma}_h - \mathbf{b}u_h)\|_{0,\kappa}^2 + \|\Lambda_h u_h - u_h\|_0^2 \right. \\ &\quad \left. + \|\Lambda_h u_h - u\|_0^2 + |\lambda - \lambda_h|^2 + \sum_{E \in \Gamma(\kappa)} h_\kappa^2 \|J_F\|_{0,E}^2 \right\}^{\frac{1}{2}}. \end{aligned}$$

The proof is complete

### 5.7 Effectiveness Of The Characteristic Function Estimator

The next objective is to prove that the local error estimator indicator  $\eta_\kappa$  gives a local lower bound for the error on element  $\kappa$ , in order to confirm the effectiveness of our estimation approach in practical adaptive refinement. Let  $b_\kappa \in H_0^1(\kappa)$  denote the standard element bubble function, and  $b_E \in H_0^1(U_E)$  denote the bubble function on the face. Here,  $U_E$  is the union of two elements  $\kappa^+$  and  $\kappa^-$  sharing the edge  $E$ . We sort the vertices of  $\kappa^+$  and  $\kappa^-$  such that the vertices of the edge  $E$  are listed first. Define  $b_E$  as follows

$$b_E = \begin{cases} 4\lambda_{\kappa^+}\lambda_{\kappa^-}, & \text{on } \kappa^+ \text{ or } \kappa^-, \\ 0, & \text{on } \Omega/U_E. \end{cases}$$

**Lemma 5.8.** (Properties of Bubble Functions) Let  $\kappa \in \mathcal{T}_h$  and  $E \in \Gamma_h$ , then the functions  $b_\kappa$  and  $b_E$  have the following properties:

$$\begin{aligned} \text{supp}b_\kappa &\subset \kappa, 0 \leq b_\kappa \leq 1, \max_{z \in \kappa} b_\kappa(x) = 1, \\ \text{supp}b_E &\subset \kappa, 0 \leq b_E \leq 1, \max_{z \in E} b_E(x) = 1, \\ h_\kappa^2 &\lesssim \int_\kappa b_\kappa dx = \frac{|\kappa|}{60} \lesssim h_\kappa^2, \\ h_E^2 &\lesssim \int_{\kappa'} b_E dx = \frac{|\kappa'|}{3} \lesssim h_E^2, \forall \kappa' \subset U_E \\ \|\nabla b_\kappa\|_{0,\kappa} &\lesssim h_\kappa^{-1} \|b_\kappa\|_{0,\kappa} \\ \|\nabla b_E\|_{0,\kappa'} &\lesssim h_E^{-1} \|b_\kappa\|_{0,\kappa'}, \forall \kappa' \subset U_E, \end{aligned} \tag{5.47}$$

where the mesh's shape regularity determines the hidden constants.

**Lemma 5.9.** (Inverse Inequality) Let  $l, m \in \mathbb{N} \cup \{0\}$  with  $l \leq m$ . Then, for every  $\kappa \in \mathcal{T}_h$ , we have

$$|p|_{m,\kappa} \lesssim h_\kappa^{l-m} |p|_{l,\kappa}, \forall p \in P_\kappa(\kappa),$$

where the hidden constant depends on  $k, m, l$ , and the shape regularity of the mesh.

Based on the above lemma, and combining Verfürth's bubble function technique developed with the standard parametrization method, we can prove the following local lower bounds.

**Lemma 5.10.** For any element  $\kappa \in \mathcal{T}_h$ , the following local lower bounds hold

$$(i) \text{ For any element } \kappa \in \mathcal{T}_h, \text{ we have} \quad h_\kappa^2 \|\mathbf{rot}(\boldsymbol{\sigma}_h - \mathbf{b}u_h)\|_{0,\kappa}^2 \lesssim \|\boldsymbol{\sigma} - \boldsymbol{\sigma}_h\|_{0,\kappa}^2 + \|u - u_h\|_{0,\kappa}^2 + h_\kappa^2 \text{osc}_h(\kappa)^2, \tag{5.48}$$

where

$$\text{osc}_h(\kappa) = \|\mathbf{rot}(\boldsymbol{\sigma}_h - \mathbf{b}u_h) - Q_h(\mathbf{rot}(\boldsymbol{\sigma}_h - \mathbf{b}u_h))\|_{0,\kappa}; \tag{5.49}$$

(ii) For any element  $\kappa \in \mathcal{T}_h$ , we have

$$\|\Lambda_h u_h - u_h\|_{0,\kappa}^2 \lesssim \|u - u_h\|_{0,\tilde{\omega}_\kappa}^2 + \|\Lambda_h u - u\|_{0,\kappa}^2; \tag{5.50}$$

(iii) Let  $E \in \Gamma_h$  be the internal edge shared by elements  $\kappa^+$  and  $\kappa^-$ , then we get

$$h_E \|J_F\|_{0,E}^2 \lesssim \|\boldsymbol{\sigma} - \boldsymbol{\sigma}_h\|_{0,U_E}^2 + \|u - u_h\|_{0,U_E}^2 + \sum_{\kappa \in U_E} h_\kappa^2 \text{osc}_h(\kappa)^2. \tag{5.51}$$

**Proof.** (i) First, consider the following inequality

$$\begin{aligned} h_\kappa^2 \|\mathbf{rot}(\boldsymbol{\sigma}_h - \mathbf{b}u_h)\|_{0,\kappa}^2 &\leq h_\kappa^2 \|\mathbf{rot}(\boldsymbol{\sigma}_h - \mathbf{b}u_h) - Q_h(\mathbf{rot}(\boldsymbol{\sigma}_h - \mathbf{b}u_h))\|_{0,\kappa}^2 \\ &\quad + h_\kappa^2 \|Q_h(\mathbf{rot}(\boldsymbol{\sigma}_h - \mathbf{b}u_h))\|_{0,\kappa}^2, \end{aligned} \tag{5.52}$$

Thus, the proof only requires estimating  $h_\kappa^2 \|Q_h(\mathbf{rot}(\boldsymbol{\sigma}_h - \mathbf{b}u_h))\|_{0,\kappa}^2$ .

Let  $z_\kappa^{\text{int}}$  be the midpoint of the edge  $E$  of element  $\kappa \in \mathcal{T}_h$ , and let  $b_\kappa$  be a piecewise cubic basis function on  $\kappa$ , such that  $b_\kappa(z_\kappa^{\text{int}}) = 1$ , and vanishes on  $\partial\kappa$ . Define  $p_\kappa = Q_h(\mathbf{rot}(\boldsymbol{\sigma}_h - \mathbf{b}u_h))b_\kappa$ , and use standard interpolation estimates to obtain

$$\|\mathbf{curl}p_\kappa\|_{0,\kappa} \lesssim h_\kappa^{-1} \|Q_h(\mathbf{rot}(\boldsymbol{\sigma}_h - \mathbf{b}u_h))\|_{0,\kappa}. \tag{5.53}$$

Next, From  $\mathbf{rot}(\boldsymbol{\sigma} - \mathbf{b}u) = \mathbf{rot}(\nabla u) = 0$ , the following estimate holds

$$\|Q_h(\mathbf{rot}(\boldsymbol{\sigma}_h - \mathbf{b}u_h))\|_{0,\kappa}^2 \leq \int_\kappa Q_h(\mathbf{rot}(\boldsymbol{\sigma}_h - \mathbf{b}u_h)) \cdot Q_h(\mathbf{rot}(\boldsymbol{\sigma}_h - \mathbf{b}u_h)) b_\kappa dx$$

$$\begin{aligned}
 &= \int_{\kappa} Q_h(\text{rot}(\boldsymbol{\sigma}_h - \mathbf{b}u_h)) \cdot p_{\kappa} dx \\
 &\leq C \int_{\kappa} \text{rot}(\boldsymbol{\sigma}_h - \mathbf{b}u_h) \cdot p_{\kappa} dx + \frac{1}{3} \|Q_h(\text{rot}(\boldsymbol{\sigma}_h - \mathbf{b}u_h))\|_{0,\kappa}^2 \\
 &\quad + C \|\text{rot}(\boldsymbol{\sigma}_h - \mathbf{b}u_h) - Q_h(\text{rot}(\boldsymbol{\sigma}_h - \mathbf{b}u_h))\|_{0,\kappa}^2 \\
 &\leq C \int_{\kappa} \text{rot}(\boldsymbol{\sigma}_h - \mathbf{b}u_h - \boldsymbol{\sigma} + \mathbf{b}u) \cdot p_{\kappa} dx + \frac{1}{3} \|Q_h(\text{rot}(\boldsymbol{\sigma}_h - \mathbf{b}u_h))\|_{0,\kappa}^2 \\
 &\quad + C \|\text{rot}(\boldsymbol{\sigma}_h - \mathbf{b}u_h) - Q_h(\text{rot}(\boldsymbol{\sigma}_h - \mathbf{b}u_h))\|_{0,\kappa}^2, \tag{5.54}
 \end{aligned}$$

the integral term  $\int_{\kappa} \text{rot}(\boldsymbol{\sigma}_h - \mathbf{b}u_h - \boldsymbol{\sigma} + \mathbf{b}u) \cdot p_{\kappa} dx$  can be solved using Green's formula, we get

$$\begin{aligned}
 &\int_{\kappa} \text{rot}(\boldsymbol{\sigma}_h - \mathbf{b}u_h - \boldsymbol{\sigma} + \mathbf{b}u) \cdot p_{\kappa} dx \\
 &= - \int_{\kappa} (\boldsymbol{\sigma}_h - \mathbf{b}u_h - \boldsymbol{\sigma} + \mathbf{b}u) \cdot \text{curl} p_{\kappa} dx + \int_{\partial\kappa} \mathbf{t} \cdot (\boldsymbol{\sigma}_h - \mathbf{b}u_h - \boldsymbol{\sigma} + \mathbf{b}u) \cdot p_{\kappa} dx \\
 &= \int_{\kappa} (\boldsymbol{\sigma}_h - \mathbf{b}u_h - \boldsymbol{\sigma} + \mathbf{b}u) \cdot \text{curl} p_{\kappa} dx,
 \end{aligned}$$

substitute the above into (5.54) and combine with (5.53), yielding:

$$\begin{aligned}
 &\|Q_h(\text{rot}(\boldsymbol{\sigma}_h - \mathbf{b}u_h))\|_{0,\kappa}^2 \\
 &\leq C \int_{\kappa} (\boldsymbol{\sigma}_h - \mathbf{b}u_h - \boldsymbol{\sigma} + \mathbf{b}u) \cdot \text{curl} p_{\kappa} dx + \frac{1}{3} \|Q_h(\text{rot}(\boldsymbol{\sigma}_h - \mathbf{b}u_h))\|_{0,\kappa}^2 \\
 &\quad + C \|\text{rot}(\boldsymbol{\sigma}_h - \mathbf{b}u_h) - Q_h(\text{rot}(\boldsymbol{\sigma}_h - \mathbf{b}u_h))\|_{0,\kappa}^2 \\
 &\leq C \|\text{curl} p_{\kappa}\|_{0,\kappa} \cdot (\|\boldsymbol{\sigma} - \boldsymbol{\sigma}_h\|_{0,\kappa} + \|\mathbf{b}\|_{0,\kappa} \|u - u_h\|_{0,\kappa}) \\
 &\quad + \frac{1}{3} \|Q_h(\text{rot}(\boldsymbol{\sigma}_h - \mathbf{b}u_h))\|_{0,\kappa}^2 + C \|\text{rot}(\boldsymbol{\sigma}_h - \mathbf{b}u_h) - Q_h(\text{rot}(\boldsymbol{\sigma}_h - \mathbf{b}u_h))\|_{0,\kappa}^2 \\
 &\leq Ch_{\kappa}^{-1} \|Q_h(\text{rot}(\boldsymbol{\sigma}_h - \mathbf{b}u_h))\|_{0,\kappa} \cdot (\|\boldsymbol{\sigma} - \boldsymbol{\sigma}_h\|_{0,\kappa} + \|u - u_h\|_{0,\kappa}) \\
 &\quad + \frac{1}{3} \|Q_h(\text{rot}(\boldsymbol{\sigma}_h - \mathbf{b}u_h))\|_{0,\kappa}^2 + C \|\text{rot}(\boldsymbol{\sigma}_h - \mathbf{b}u_h) - Q_h(\text{rot}(\boldsymbol{\sigma}_h - \mathbf{b}u_h))\|_{0,\kappa}^2,
 \end{aligned}$$

so it is possible to get

$$\begin{aligned}
 &\|Q_h(\text{rot}(\boldsymbol{\sigma}_h - \mathbf{b}u_h))\|_{0,\kappa}^2 \lesssim h_{\kappa}^{-2} (\|\boldsymbol{\sigma} - \boldsymbol{\sigma}_h\|_{0,\kappa}^2 + \|u - u_h\|_{0,\kappa}^2) \\
 &\quad + \|\text{rot}(\boldsymbol{\sigma}_h - \mathbf{b}u_h) - Q_h(\text{rot}(\boldsymbol{\sigma}_h - \mathbf{b}u_h))\|_{0,\kappa}^2. \tag{5.55}
 \end{aligned}$$

Finally, we obtain a proof of (i) by substituting (5.55) into (5.52).

(ii) By property (iii) of Lemma 5.3, we have

$$\begin{aligned}
 \|A_h u_h - u_h\|_{0,\kappa} &= \|A_h u_h - A_h u + A_h u + u - u - u_h\|_{0,\kappa} \\
 &\leq \|A_h(u_h - u)\|_{0,\kappa} + \|A_h u - u\|_{0,\kappa} + \|u - u_h\|_{0,\kappa} \\
 &\lesssim \|u - u_h\|_{0,\tilde{\omega}_{\kappa}} + \|A_h u - u\|_{0,\kappa}.
 \end{aligned}$$

Hence, we get

$$\|A_h u_h - u_h\|_{0,\kappa}^2 \lesssim \|u - u_h\|_{0,\tilde{\omega}_{\kappa}}^2 + \|A_h u - u\|_{0,\kappa}^2.$$

(iii) Let  $E \in \Gamma_h$  be an interior edge shared by the boundaries  $\kappa^+$  and  $\kappa^-$ , and let  $p_E$  satisfy  $\text{supp } p_E \subset U_E$ . We define  $b_E$  as a piecewise quadratic basis function on  $U_E$  which is equal to one at the midpoint of  $U_E$  and vanishes on  $\partial U_E$ .

Define  $p_E = \delta J_F b_E$ , where the constant  $\delta$  is defined as

$$\delta = \int_E J_F^2 h_E ds / \int_E J_F^2 b_E ds,$$

this gives the following relationship

$$\int_E J_F p_E ds = h_E \|J_F\|_{0,E}^2. \tag{5.56}$$

Thus, estimating  $h_E \|J_F\|_{0,E}^2$  is equivalent to estimating  $\int_E J_F p_E ds$ . According to standard theory,  $\delta \lesssim h_E$ . Furthermore, by inverse estimates, we obtain the following inequalities (see [13])

$$\|p_E\|_{1,U_E} \lesssim h_E^{1/2} \|J_F\|_{0,E}, \tag{5.57}$$

$$\|p_E\|_{0,U_E} \lesssim h_E^{3/2} \|J_F\|_{0,E}. \tag{5.58}$$

Furthermore, since

$$\int_{\kappa} \text{rot}(\boldsymbol{\sigma}_h - \mathbf{b}u_h) \cdot p_E dx = \int_{\kappa} \text{rot}(\boldsymbol{\sigma}_h - \boldsymbol{\sigma} + \mathbf{b}u - \mathbf{b}u_h) \cdot p_E dx,$$

we apply Green's formula to the latter expression, getting

$$\begin{aligned} & \int_{\kappa} \text{rot}(\boldsymbol{\sigma}_h - \boldsymbol{\sigma} + \mathbf{b}u - \mathbf{b}u_h) \cdot p_E dx \\ &= \int_{\kappa} (\boldsymbol{\sigma}_h - \boldsymbol{\sigma} + \mathbf{b}u - \mathbf{b}u_h) \cdot \mathbf{curl} p_E dx - \int_{\partial\kappa} (\boldsymbol{\sigma}_h - \boldsymbol{\sigma} + \mathbf{b}u - \mathbf{b}u_h) \cdot \mathbf{t} \cdot p_E ds \\ &= \int_{\kappa} (\boldsymbol{\sigma}_h - \boldsymbol{\sigma} + \mathbf{b}u - \mathbf{b}u_h) \cdot \mathbf{curl} p_E dx - \int_{\partial\kappa} (\boldsymbol{\sigma}_h - \mathbf{b}u_h) \cdot \mathbf{t} \cdot p_E ds + \int_{\partial\kappa} (\boldsymbol{\sigma} - \mathbf{b}u) \cdot \mathbf{t} \cdot p_E ds \\ &= \int_{\kappa} (\boldsymbol{\sigma}_h - \boldsymbol{\sigma} + \mathbf{b}u - \mathbf{b}u_h) \cdot \mathbf{curl} p_E dx - \int_{\partial\kappa} (\boldsymbol{\sigma}_h - \mathbf{b}u_h) \cdot \mathbf{t} \cdot p_E ds. \end{aligned}$$

Thus, we get

$$\begin{aligned} \int_E J_F p_E ds &= \int_{U_E} (\boldsymbol{\sigma}_h - \boldsymbol{\sigma}) \cdot \mathbf{curl} p_E dx + \int_{\kappa} (\mathbf{b}u - \mathbf{b}u_h) \cdot \mathbf{curl} p_E dx \\ &\quad - \sum_{\kappa \in U_E} \int_{\kappa} \text{rot}(\mathbf{b}u - \mathbf{b}u_h) \cdot p_E dx. \end{aligned} \tag{5.59}$$

The combination of (5.56)-(5.59) gives

$$\begin{aligned} h_E \|J_F\|_{0,E}^2 &= \int_E J_F p_E ds \\ &\lesssim \|\boldsymbol{\sigma} - \boldsymbol{\sigma}_h\|_{0,U_E} \cdot \|\mathbf{curl} p_E\|_{0,U_E} + \|u - u_h\|_{0,U_E} \cdot \|\mathbf{curl} p_E\|_{0,U_E} + \sum_{\kappa \in U_E} \|\text{rot}(\boldsymbol{\sigma}_h - \mathbf{b}u_h)\|_{0,\kappa} \cdot \|p_E\|_{0,\kappa} \\ &\lesssim \|\boldsymbol{\sigma} - \boldsymbol{\sigma}_h\|_{0,U_E} \cdot h_E^{1/2} \|J_F\|_{0,E} + \|u - u_h\|_{0,U_E} \cdot h_E^{1/2} \|J_F\|_{0,E} + \sum_{\kappa \in U_E} \|\text{rot}(\boldsymbol{\sigma}_h - \mathbf{b}u_h)\|_{0,\kappa} \cdot h_E^{2/3} \|J_F\|_{0,E}, \end{aligned}$$

thus, we obtain

$$h_E^{1/2} \|J_F\|_{0,E} \lesssim \|\boldsymbol{\sigma} - \boldsymbol{\sigma}_h\|_{0,U_E} + \|u - u_h\|_{0,U_E} + h_E \|\text{rot}(\boldsymbol{\sigma}_h - \mathbf{b}u_h)\|_{0,U_E},$$

squaring both sides gives

$$h_E \|J_F\|_{0,E}^2 \lesssim \|\boldsymbol{\sigma} - \boldsymbol{\sigma}_h\|_{0,U_E}^2 + \|u - u_h\|_{0,U_E}^2 + h_E^2 \|\text{rot}(\boldsymbol{\sigma}_h - \mathbf{b}u_h)\|_{0,U_E}^2, \tag{5.60}$$

substituting (5.48) into (5.60) leads (5.51).

The following result is obtained using Lemma 5.11 and the specification of the local error estimator  $\eta_{\kappa}$ .

**Theorem 5.3.** Let  $(\lambda, \boldsymbol{\sigma}, u)$  be the solution of (3.3), and  $(\lambda_h, \boldsymbol{\sigma}_h, u_h)$  be the solution of (4.1). Then, there exists  $h_0$ , such that for all  $h < h_0$ , the following inequality holds:

$$\eta_{\kappa}^2 \lesssim \|\boldsymbol{\sigma} - \boldsymbol{\sigma}_h\|_{0,\omega_{\kappa}}^2 + \|u - u_h\|_{0,\tilde{\omega}_{\kappa}}^2 + \|A_h u - u\|_{0,\kappa}^2 + \|c - Q_h c\|_{0,\kappa}^2 + \sum_{\kappa \in \omega_{\kappa}} h_{\kappa}^2 \text{osc}_h(\kappa)^2.$$

where  $\|A_h u - u\|_{0,\kappa}^2$  are the higher-order terms.

**Proof.** Substituting the conditions (i)-(iii) into (5.34), the conclusion follows immediately.

## VI. NUMERICAL EXPERIMENTS

In this section, the effectiveness of our method is validated through a series of numerical experiments by compiling the code under the iFEM package. Here we give the numerical results of the adaptive mixed finite element algorithm for the first eigenpair approximation with the parameter  $\theta = 0.4$ . We consider problem (3.1), where we take  $\mathbf{b} = (0,0)^T, (3,0)^T, (1 + 2i, 1 + 2i)^T$ , and  $c = 0, 0, i$ . Additionally, we consider a more general eigenvalue problem, where  $\mathbf{b} = (1 + (x - 1/2)^2, (x - 1/2)(y - 1/2))^T$  and  $c = e^{(x-1/2)(y-1/2)}$ .

In this experiment, we primarily compute for two test domains: the L-shaped domain  $\Omega_L = (-1,1)^2 \setminus ([0,1] \times (-1,0])$ , and the crack structure domain  $\Omega_{SL} = (-1,1)^2 \setminus \{0 \leq x \leq 1, y = 0\}$ . Since the exact eigenvalues are unknown, we select eight sufficiently accurate approximate values as the reference for the numerical test. These reference eigenvalues are obtained as accurately as possible through adaptive computations. The specific results are as follows:

**Table 1** When  $\mathbf{b} = (0,0)^T$  and  $c = 0$ , the numerical solution for the eigenvalues for regions  $\Omega_L, \Omega_{SL}$ .

Domain	ref	$\ell$	$h$	$\lambda_1$	dof	Error	rate
$\Omega_L$	9.6397238440219	15	1/4	9.590522	4178	0.049202	1.576941
		15	1/8	9.623232	14574	0.016492	1.708429
		15	1/16	9.634677	54482	0.005046	1.673099
		15	1/32	9.638141	217294	0.001582	1.488397
		15	1/64	9.639160	863271	0.000564	1.990692

Domain	ref	$\ell$	$h$	$\lambda_1$	dof	Error	rate
		15	1/128	9.639582	3448507	0.000142	
$\Omega_{SL}$	8.3713297112	15	1/4	8.260351	5065	0.110979	1.706567
		15	1/8	8.337327	20464	0.034003	1.120043
		15	1/16	8.355686	73936	0.015644	1.522870
		15	1/32	8.365886	289187	0.005444	1.734294
		15	1/64	8.369693	1148872	0.001636	1.663791
		15	1/128	8.370813	4578960	0.000516	

Table 2 When  $\mathbf{b} = (3,0)^T$  and  $c = 0$ , the numerical solution for the eigenvalues for regions  $\Omega_L, \Omega_{SL}$ .

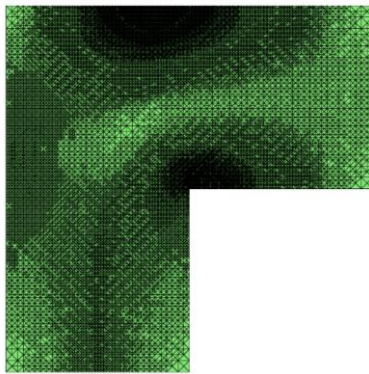
Domain	ref	$\ell$	$h$	$\lambda_1$	dof	Error	rate
$\Omega_L$	11.88972384472	16	1/4	11.833583	4546	0.056141	0.626876
		16	1/8	11.853368	15212	0.036355	1.645681
		16	1/16	11.878105	57354	0.011619	1.876514
		16	1/32	11.886560	218654	0.003164	1.790759
		16	1/64	11.888809	859561	0.000915	1.803418
		16	1/128	11.889462	3411582	0.000262	
$\Omega_{SL}$	10.6213297112	18	1/4	10.470400	6445	0.150930	1.394947
		18	1/8	10.563937	24801	0.057392	1.293193
		18	1/16	10.597911	96820	0.023419	1.566618
		18	1/32	10.613424	377098	0.007906	1.560939
		18	1/64	10.618650	1486399	0.002680	1.488930
		18	1/128	10.620375	5869239	0.000955	

Table 3 When  $\mathbf{b} = (1 + 2i, 1 + 2i)^T$  and  $c = i$ , the numerical solution for the eigenvalues for regions  $\Omega_L, \Omega_{SL}$ .

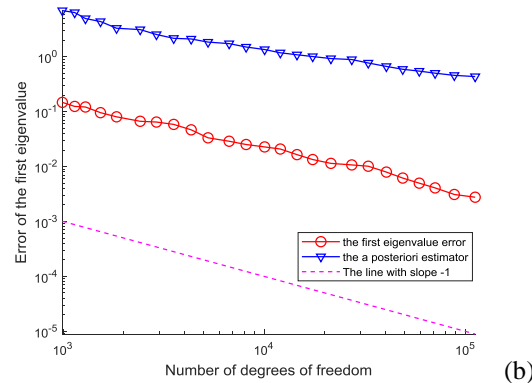
Domain	ref	$\ell$	$h$	$\lambda_1$	dof	Error	rate
$\Omega_L$	8.138884555715604 +2.999945254673094i	11	1/4	8.055754 +2.982357i	1840	0.084971	1.835314
		11	1/8	8.115430 +2.995781i	7669	0.023822	1.719882
		11	1/16	8.131714 +2.998972i	33633	0.007237	2.414813
		11	1/32	8.137538 +2.999775i	156688	0.001357	2.830166
		11	1/64	8.139075 +2.999955i	741736	1.911166E-04	
		$\Omega_{SL}$	6.866940231816318 +2.999950742707009i	10	1/4	6.621008 +2.989043i	1836
10	1/8			6.796031 +2.996494i	7743	0.070993	1.134078
10	1/16			6.834590 +2.999186i	34623	0.032359	2.252026
10	1/32			6.860148 ++2.999825i	161270	0.006793	

**Table 4** When  $\mathbf{b} = (1 + (x - 1/2)^2, (x - 1/2)(y - 1/2))^T$  and  $c = e^{(x-1/2)(y-1/2)}$ , the numerical solution for the eigenvalues for regions  $\Omega_L, \Omega_{SL}$ .

Domain	ref	$\ell$	$h$	$\lambda_1$	dof	Error	rate
$\Omega_L$	11.4325182548738	9	1/4	11.250697	1219	0.181821	1.558814
		9	1/8	11.370803	4502	0.061716	1.494713
		9	1/16	11.410618	16963	0.021900	2.085843
		9	1/32	11.427360	67521	0.005159	2.381284
		9	1/64	11.431528	279292	0.000990	
Domain	ref	$\ell$	$h$	$\lambda_1$	dof	Error	rate
$\Omega_{SL}$	10.0036912872557	8	1/4	9.573823	914	0.429868	1.209399
		8	1/8	9.817795	3952	0.185896	1.927018
		8	1/16	9.954806	15465	0.048885	1.723604
		8	1/32	9.988889	64277	0.014802	2.142861
		8	1/64	10.000340	269944	0.003352	1.492321
		8	1/128	10.004883	1162925	0.001191	

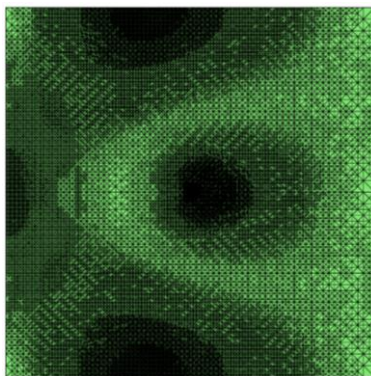


(a)

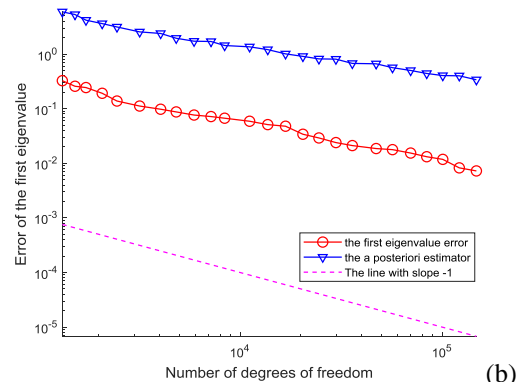


(b)

**Figure 1:** When  $\mathbf{b} = (0,0)^T$  and  $c = 0$ , the adaptive mesh and error curve plot on the initial grid 1/8 for the test domain  $\Omega_L$ . (a) Mesh after 25 iterations; (b) The error curve plot.



(a)



(b)

**Figure 2:** When  $\mathbf{b} = (0,0)^T$  and  $c = 0$ , the adaptive mesh and error curve plot on the initial grid 1/8 for the test domain  $\Omega_{SL}$ . (a) Mesh after 25 iterations; (b) The error curve plot.

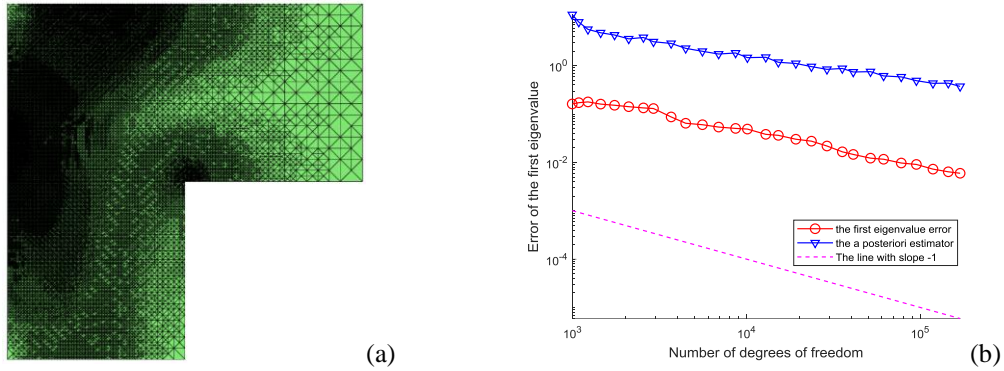


**Figure 3:** When  $\mathbf{b} = (3,0)^T$  and  $c = 0$ , the adaptive mesh and error curve plot on the initial grid  $1/8$  for the test domain  $\Omega_L$ . (a) Mesh after 28 iterations; (b) The error curve plot.

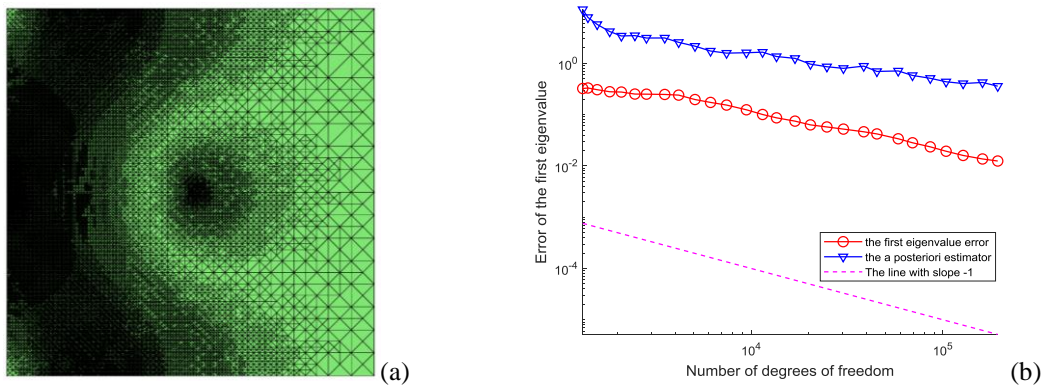


**Figure 4:** When  $\mathbf{b} = (3,0)^T$  and  $c = 0$ , the adaptive mesh and error curve plot on the initial grid  $1/8$  for the test domain  $\Omega_{SL}$ . (a) Mesh after 28 iterations; (b) The error curve plot.

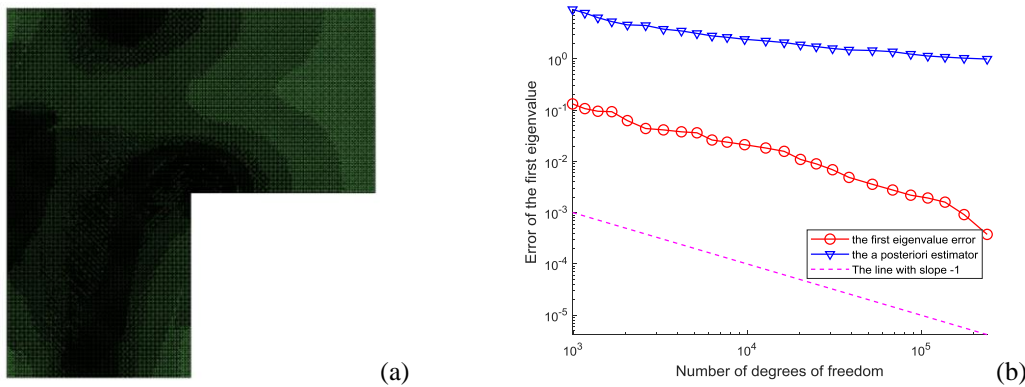


**Figure 5:** When  $\mathbf{b} = (1 + 2i, 1 + 2i)^T$  and  $c = i$ , the adaptive mesh and error curve plot on the initial grid  $1/8$  for the test domain  $\Omega_L$ . (a) Mesh after 25 iterations; (b) The error curve plot.

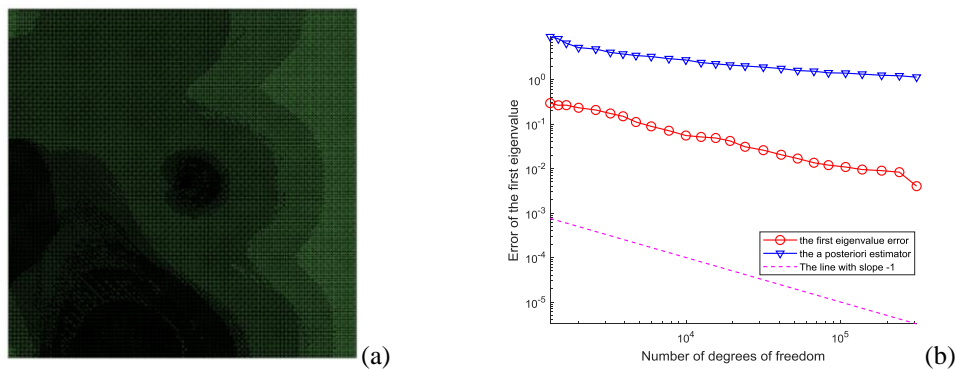


**Figure 6:** When  $\mathbf{b} = (1 + 2i, 1 + 2i)^T$  and  $c = i$ , the adaptive mesh and error curve plot on the initial grid  $1/8$  for the test domain  $\Omega_{SL}$ . (a) Mesh after 25 iterations; (b) The error curve plot.



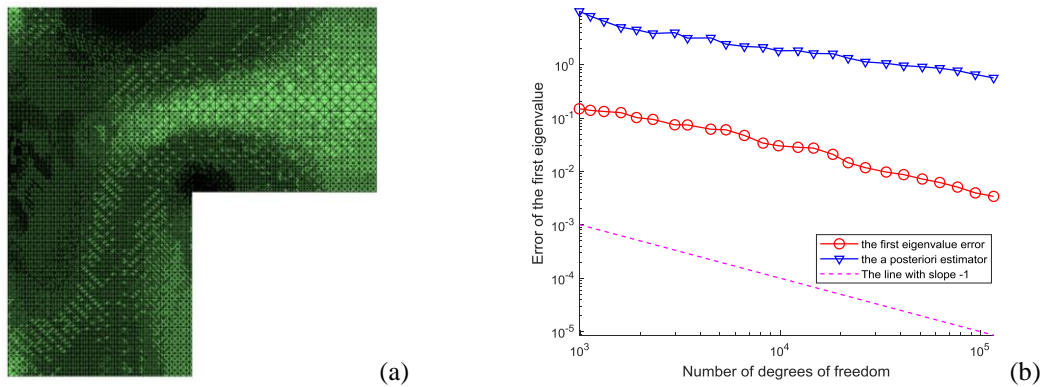


**Figure 7:** When  $\mathbf{b} = (1 + (x - 1/2)^2, (x - 1/2)(y - 1/2))^T$  and  $c = e^{(x-1/2)(y-1/2)}$ , the adaptive mesh and error curve plot on the initial grid 1/8 for the test domain  $\Omega_L$ . (a) Mesh after 25 iterations; (b) The error curve plot.

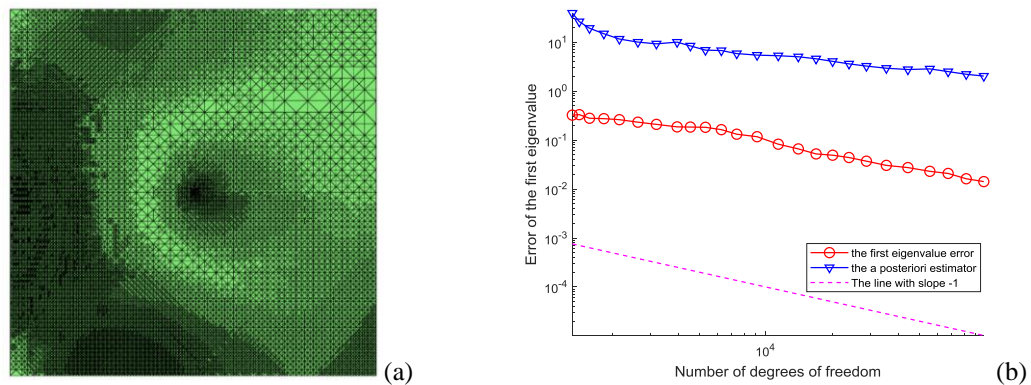


**Figure 8:** When  $\mathbf{b} = (1 + (x - 1/2)^2, (x - 1/2)(y - 1/2))^T$  and  $c = e^{(x-1/2)(y-1/2)}$ , the adaptive mesh and error curve plot on the initial grid 1/8 for the test domain  $\Omega_{SL}$ . (a) Mesh after 25 iterations; (b) The error curve plot.

## VII. CONCLUSION

In Tables 1 to 4, we present the numerical solutions of the eigenvalues obtained through adaptive computations and show the adaptive mesh and error curves in the figures. From Figures 1 to 8, it can be seen that when

$$\mathbf{b} = (0,0)^T, (3,0)^T, (1 + 2i, 1 + 2i)^T, (1 + (x - 1/2)^2, (x - 1/2)(y - 1/2))^T$$

and

$$c = 0, 0, i, e^{(x-1/2)(y-1/2)},$$

the error curves of the lowest-order Raviart-Thomas mixed finite element are approximately parallel to a straight line with a slope of -1. The results indicate that the adaptive algorithm achieves optimal convergence order.

## REFERENCES

- [1] Jim Douglas, Jr. and Jean E. Roberts, Global estimates for mixed methods for second-order elliptic equations[J]. *Mathematics of Computation*, 1985, 44 (169): 39-52.
- [2] Lin Q, Xie H. Asymptotic error expansion and Richardson extrapolation of eigenvalue approximations for second order elliptic problems by the mixed finite element method[J]. *Applied Numerical Mathematics*, 2009, 59 (8): 1884-1893.
- [3] Mingduan Liang, Ying Han, Mei Yu, hp Local Discontinuous Galerkin Finite Element Method Based on Steklov Eigenvalue Problem[J]. *International Journal of Scientific Engineering and Science*, 2024, 8 (3): 01-08.
- [4] Jia S, Chen H, Xie H. A posteriori error estimator for eigenvalue problems by mixed finite element method[J]. *Science China Mathematics*, 2013, 56 (5): 887-900.
- [5] R. Durán, L. Gastaldi, C. Padra, A posteriori error estimators for mixed approximations of eigenvalue problems[J]. *Mathematical Models and Methods in Applied Sciences*, 1999, 9 (8): 1165-1178.
- [6] 段丽梅, 陈兴龙, 韩家宇. 对流扩散特征值问题的自适应间断有限元方法[J]. *数学杂志*, 2023, 43 (06): 515-528.
- [7] Babuška, J. Osborn, Eigenvalue problems, in: P.G. Lions, P.G. Ciarlet (Eds.), *Handbook of Numerical Analysis*, vol. II, Finite Element Methods (Part 1). North-Holland, Amsterdam, 1991, pp. 641-787.
- [8] Brezzi F, Fortin M, *Mixed and Hybrid Finite Element Methods*[D]. Springer-Verlag, 1991, pp. 89-132.
- [9] B. Mercier, J. Osborn, J. Rappaz, P.A. Raviart, Eigenvalue approximation by mixed and hybrid methods[J]. *Mathematics of Computation*, 1981, 36 (154): 427-453.

- [10] Logg, G.N. Wells, DOLFIN: Automated finite element computing[J]. ACM Trans. Math. Software, 2010, 37 (2): 01-20.
- [11] Felipe L, Jesus V. A posteriori analysis for a mixed formulation of the Stokes spectral problem[J]. Calcolo, 2023, 60 (4): 01-28.
- [12] Koelink, E., vanNeerven, J.M., dePagter, B., Sweers, G., Partial Differential Equations and Functional Analysis: the Philippe Clément Festschrift. Springer, Berlin, 2006.
- [13] Mekchay K., Nochetto H.R., Convergence of Adaptive Finite Element Methods for General Second Order Linear Elliptic PDEs[J]. SIAM J. Numerical Analysis, 2005, 43 (5): 1803-1827.
- [14] 罗贤兵. 二阶椭圆本征值问题Raviart-Thomas混合有限元法的误差分析[J]. 数学杂志, 2009, 29 (01): 109-113.